

# Capacity and Optimal Resource Allocation for IRS-assisted Multi-user Communication Systems

Xidong Mu, *Student Member, IEEE*, Yuanwei Liu, *Senior Member, IEEE*,

Li Guo, *Member, IEEE*, Jiaru Lin, *Member, IEEE*, and

Naofal Al-Dhahir, *Fellow, IEEE*

## Abstract

This paper investigates intelligent reflecting surface (IRS)-assisted multi-user wireless communication systems, where an access point (AP) sends independent information to multiple users with the aid of one IRS. To determine the fundamental rate limits of these systems, we jointly optimize the IRS discrete phase-shift matrix and resource allocation for both orthogonal multiple access (OMA) and capacity-achieving non-orthogonal multiple access (NOMA) transmission schemes. The ergodic and delay-limited rate/capacity regions are characterized by invoking rate-profile techniques. For ergodic rate/capacity regions, as the formulated non-convex average sum rate maximization problems satisfy the time-sharing condition, we derive the optimal solutions for both transmission schemes using the Lagrange duality method. For OMA transmissions, the optimal solution unveils that each user should be alternatively served with its effective channel gain maximized by dynamically adjusting the IRS phase. For the NOMA transmission, the optimal transmission strategy still follows the alternative transmission scheme but among different user groups. For delay-limited rate/capacity regions, the instantaneous sum rate maximization problem is decomposed into a series of resource allocation subproblems. For OMA transmissions, we derive the optimal resource allocation by utilizing the Lagrange duality method. For NOMA transmissions, we show that the subproblem can be optimally solved by successively checking problem feasibility with the bisection method. The optimal solutions indicate that the IRS phase should be fixed throughout the transmission to maintain the instantaneous achievable rate of all users. We further propose a Hadamard codebook based scheme for IRS phase adjustment, which serves as a lower bound on the optimal performance gains. Finally, numerical results demonstrate that: i) the IRS is capable

Part of this work has been submitted to the IEEE International Conference on Communications Workshop on NOMA for 5G and Beyond, Dublin, Ireland, June 7-11, 2020. [1]

X. Mu, L. Guo, and J. Lin are with Beijing University of Posts and Telecommunications, Beijing, China. (email:{muxidong, guoli, jrlin}@bupt.edu.cn).

Y. Liu is with Queen Mary University of London, London, UK. (email:yuanwei.liu@qmul.ac.uk).

N. Al-Dhahir is with the Department of Electrical and Computer Engineering, The University of Texas at Dallas, Richardson, TX 75080 USA. (e-mail: aldhahir@utdallas.edu).

of significantly improving both the ergodic and delay-limited capacity regions; ii) the capacity region achieved by the Hadamard codebook based scheme is close to that of discrete phase shifts for a small number of IRS elements.

### **Index Terms**

Capacity region, intelligent reflecting surface, resource allocation, non-orthogonal multiple access.

## I. INTRODUCTION

The rapid development of various advanced applications (e.g., extended reality, autonomous driving, etc.) imposes more requirements on the fifth-generation (5G) and beyond wireless networks, including higher data rate, lower latency and higher reliability [2]. To meet those requirements, a variety of wireless technologies have been proposed, such as massive multiple-input multiple-output (MIMO) and millimeter-wave (mmWave) communications [3]. Despite achieving significant performance gains, these technologies also require higher hardware cost and energy consumption. To this end, intelligent reflecting surface (IRS) is emerging as a promising cost-effective and green solution [4–6].

IRS (also referred to as reconfigurable intelligent surface (RIS)) technology has drawn tremendous attention from both academia and industry. An IRS is a planar array, which consists of a large number of passive reflecting elements. Each element can passively reflect the incident electromagnetic wave while changing its amplitude and phase shift [4, 5]. With an IRS smart controller, the reflected signal propagation can be artificially changed to enhance the network performance. For instance, if the transmitter and receiver are blocked by an obstacle, an extra path can be created with the deployment of the low-cost IRS.

Non-orthogonal multiple access (NOMA) is a promising candidate technology for next-generation wireless communication networks [7]. Different from orthogonal multiple access (OMA), NOMA allows multiple users to share the same time/frequency/code resource block, where superposition coding (SC) and successive interference cancellation (SIC) are performed at the transmitter and receivers, respectively [8]. Therefore, NOMA is capable of achieving higher spectral efficiency (SE) and supporting massive connectivity [9].

### *A. Prior Works*

The performance gain of IRS has been investigated under different objectives and application scenarios. For example, Wu *et al.* [10] minimized the total transmit power by alternatively optimizing the active beamforming at the access point (AP) and the passive beamforming at the IRS. An IRS power consumption model was proposed by Huang *et al.* [11], where the energy efficiency (EE) was maximized for an IRS-assisted downlink multi-user network. With the aim

of achieving secrecy transmission, Chen *et al.* [12] proposed to deploy the IRS in a downlink multiple-input single-output (MISO) system coexisting with multiple eavesdroppers, where the passive beamforming was designed under different practical IRS elements constraints. Yu *et al.* [13] investigated IRS-assisted secure communication with imperfect channel state information (CSI). Yang *et al.* [14] proposed a dynamic passive beamforming scheme to maximize the minimum rate in an IRS-enhanced orthogonal frequency division multiple access (OFDMA) network. The channel capacity of an IRS-assisted MIMO system was maximized by Zhang *et al.* [15], where alternating optimization algorithms were proposed under frequency-flat and frequency-selective channels. In [16], IRS performance gains were analyzed in a MIMO communication network. The effectiveness of the IRS was evaluated in [17] via experimental tests at 2.3 GHz and 28.5 GHz.

Significant efforts have been devoted to investigate NOMA technology in the past few years. For instance, the sum rate and outage performances of NOMA were analyzed by Ding *et al.* [18] with different user pairing schemes in both fixed power allocation NOMA (F-NOMA) and cognitive radio inspired NOMA (CR-NOMA) systems. Yang *et al.* [18] further propose a dynamic power allocation scheme (D-NOMA) whose performance outperforms that of F-NOMA and CR-NOMA. In terms of the sum rate performance, the superiority of NOMA over OMA was mathematically proved by Chen *et al.* [19]. Furthermore, the performance gains of NOMA were studied in numerous scenarios, such as physical layer security [20], mmWave communication [21] and heterogeneous networks (HetNets) [22].

To further improve the system performance, some initial studies have focused on the integration of IRS and NOMA technologies. In [23], IRSs were used to enhance the received signal strength of cell-edge users in NOMA transmission. The max-min rate problem in the IRS-NOMA network was investigated by Yang *et al.* [24]. Fu *et al.* [25] minimized the transmit power in a downlink IRS-assisted MISO system, where an efficient difference-of-convex (DC) based algorithm was proposed for passive beamforming designs. The sum rate of all users in an IRS-NOMA network was maximized in [26] with ideal and non-ideal IRS elements. Moreover, Zhu *et al.* [27] designed the passive beamforming with the concept of quasi-degradation condition and proposed a hybrid NOMA transmission scheme. Hou *et al.* [28] analyzed SE and EE performance of the IRS-assisted NOMA network with a priority based design.

### B. Motivations and Contributions

Despite the fact that there are growing research efforts to study the performance enhancement due to IRS, there are limited works on characterizing the capacity of IRS-assisted multi-user systems. To the best of our knowledge, there is only one prior work [15] that studied the capacity limits of IRS-assisted systems, where the capacity was maximized for an IRS-assisted point-to-point MIMO system. However, the results in [15] cannot be applied for the multi-user scenario. The optimal capacity-achieving transmission strategies and resource allocation schemes for IRS-assisted multi-user communication systems remain unknown, which motivates this work.

We investigate IRS-assisted multi-user communication systems where a single-antenna AP sends independent information to multiple single-antenna users with the aid of one IRS. For practical implementation, the IRS uses discrete phase shifts. Under this setup, we jointly optimize the IRS phase-shift matrix as well as resource allocation to reveal the fundamental rate limits of IRS-assisted multi-user communication systems. The main contributions of this paper are as follows:

- We characterize the ergodic and delay-limited rate/capacity regions for both OMA and capacity-achieving NOMA schemes. By utilizing the rate-profile technique, the Pareto boundary of these regions can be characterized by maximizing the sum rate of all users, subject to a set of rate-profile constraints, discrete IRS phase shifts and resource allocation constraints.
- For ergodic rate and capacity regions, the formulated problems for both transmission schemes are shown to satisfy the time-sharing condition [29]. We can find the optimal solutions using the Lagrange duality method. The derived optimal solutions reveal that the optimal transmission strategy is carrying out alternative transmission among different users for OMA and among different user groups for NOMA by dynamically adjusting the IRS phases.
- For delay-limited rate and capacity regions, the Pareto boundary is characterized by solving a series of instantaneous sum rate maximization subproblem under a given IRS phase-shift matrix. The optimal power and orthogonal resource allocation solutions for OMA are obtained by invoking the Lagrange duality method. The optimal power allocation for NOMA is derived by checking the feasibility of a sequence of convex power minimization problems. Furthermore, a low complexity Hadamard codebook based scheme is further proposed for all schemes, which provides a lower bound on the optimal performance gains.
- Numerical results show that 1) both the ergodic and delay-limited capacity regions achieved by introducing the IRS are significantly larger than those without the IRS; 2) the proposed

Hadamard codebook based scheme can achieve a near optimal performance for a small number of IRS elements; 3) the performance gain of NOMA over OMA in the IRS-assisted system outperforms than that without the IRS.

### C. Organization and Notations

The rest of this paper is organized as follows. Section II presents the system model of the IRS-assisted multi-user communication system and the two transmission schemes. Then, we characterize the Pareto boundary of the ergodic and delay-limited capacity regions in Section III and Section IV, respectively. Section V presents numerical results to demonstrate the performance of our proposed designs and compare them with other benchmark schemes. Finally, Section VI concludes the paper.

*Notations:* Scalars are denoted by lower-case letters. Vectors and matrices are denoted by bold-face lower-case and upper-case letters, respectively.  $\mathbb{C}^{N \times 1}$  denotes the space of  $N \times 1$  complex-valued vectors.  $\mathbf{a}^T$ ,  $\mathbf{a}^H$  and  $\text{diag}(\mathbf{a})$  denote the transpose, the conjugate transpose and the diagonal matrix of vector  $\mathbf{a}$ , respectively.

## II. SYSTEM MODEL AND TRANSMISSION SCHEMES

### A. System Model

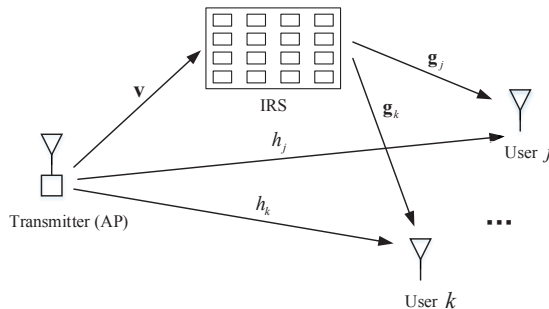


Fig. 1: Illustration of the IRS-assisted multi-user communication system.

As shown in Fig.1, we consider an IRS-assisted multi-user communication system, where a single-antenna AP transmits independent information to  $K$  single-antenna users with the aid of an IRS equipped with  $M$  passive reflecting elements. Let  $\mathbf{v} \in \mathbb{C}^{M \times 1}$  and  $h_k$  denote the corresponding AP-IRS channel and that between the AP and user  $k$ . In addition, the channel between the IRS and user  $k$  is denoted by  $\mathbf{g}_k \in \mathbb{C}^{M \times 1}$ . In this paper, we assume that all channels follow the quasi-static block fading channel model [14, 30], where the channel condition remains approximately constant in each channel coherence block. To reveal the most essential design

insights and for ease of exposition, we focus on one specific channel coherence block and let  $T$  denote the block duration<sup>1</sup>. Therefore, at each time instant  $t \in \mathcal{T} \triangleq [0, T]$ , the IRS's diagonal phase-shift matrix is denoted by  $\Theta(t) = \text{diag}(\beta_1(t) e^{j\theta_1(t)}, \beta_2(t) e^{j\theta_2(t)}, \dots, \beta_M(t) e^{j\theta_M(t)})$ , where  $\beta_m(t)$  and  $\theta_m(t) \in [0, 2\pi)$  are the instant amplitude and phase shift coefficients of the  $m$ th IRS element, respectively. For practical implementation, we assume a finite resolution phase shift for each IRS element, which has a constant reflection amplitude (e.g.,  $\beta_m(t) = 1, \forall t, m$ ) and discrete phase values  $\mathcal{D} \triangleq \{\frac{n2\pi}{L}, n = 0, 1, 2, \dots, L-1\}$ , where  $L = 2^B$  and  $B$  denotes the number of bits to adjust the phase. Let  $\mathcal{S}$  denote the set of all possible phase-shift matrices at the IRS and  $|\mathcal{S}| \triangleq L^M$ .

To characterize the capacity region with the IRS, we assume that the CSI of all channels involved can be perfectly obtained at the AP. The combined channel gain from the AP to user  $k$  at time instant  $t$  is given by  $|h_k + \mathbf{g}_k^H \Theta(t) \mathbf{v}|^2$ . We denote by  $s_k(t)$  and  $p_k(t)$  the transmitted information-bearing signal and the transmit power for user  $k$  at time instant  $t$ , respectively. Therefore, the received signal at user  $k$  at time instant  $t$  can be expressed as

$$y_k(t) = (h_k + \mathbf{g}_k^H \Theta(t) \mathbf{v}) \sum_{k=1}^K \sqrt{p_k(t)} s_k(t) + n_k(t), \quad (1)$$

where  $n_k(t)$  is the additive white Gaussian noise (AWGN) at user  $k$ . For ease of exposition, the noise power of each user is assumed to be equal to  $\sigma^2$  and the instantaneous power constraint at the AP is considered. Let  $P_{max}$  denote the maximum transmit power constraint at each time instant  $t$ , then we have  $\sum_{k=1}^K p_k(t) \leq P_{max}, \forall t$ . With the aim of achieving the capacity region of this channel, the AP should employ Gaussian signaling by setting  $s_k(t)$ 's as independent circularly symmetric complex Gaussian (CSCG) random variables with zero mean and unit variances  $\mathbb{E}(|s_k(t)|^2) = 1, \forall k$ .

### B. OMA Transmission Scheme

For the OMA transmission scheme, e.g., frequency division multiple access (FDMA) or time division multiple access (TDMA), the  $k$ th user receives its information  $s_k(t)$  with the transmit power  $p_k(t)$  over  $\omega_k(t) \in [0, 1]$  of the total orthogonal resources (time/frequency) at time instant  $t$ , where  $\sum_{k=1}^K \omega_k(t) \leq 1, \forall t$ . Then, the instantaneous achievable rate in bits per second per Hertz (bit/s/Hz) of user  $k$  in the OMA scheme can be expressed as

$$R_k^O(t) = \omega_k(t) \log_2 \left( 1 + \frac{|h_k + \mathbf{g}_k^H \Theta(t) \mathbf{v}|^2 p_k(t)}{\omega_k(t) \sigma^2} \right) \quad (2)$$

<sup>1</sup>In this paper, we assume that the users are static or moving slowly. Therefore, the channels might stay the same for a quite long time period  $T$  and the time for adjusting the IRS phase can be ignored. The case with conventional fading channels leaves as our future works.

Note that the expression in (2) is applicable to both FDMA and TDMA scenarios since the instantaneous consumed energy in TDMA (given by  $\sum_{k=1}^K \omega_k(t) \frac{p_k(t)}{\omega_k(t)}$ ) is the same as that in FDMA (given by  $\sum_{k=1}^K p_k(t)$ ). Moreover, the average achievable rate of user  $k$  over the entire period  $T$  in the OMA scheme is given by  $\bar{R}_k^O = \frac{1}{T} \int_0^T R_k^O(t) dt$ .

**Remark 1.** For OMA transmissions, in this paper, we assume that the orthogonal resources (time/frequency) are allocated in an adaptive manner. For conventional OMA transmissions, time/frequency resources are equally allocated, which is provided as a benchmark scheme in Section V.

### C. NOMA Transmission Scheme

Next, we consider the capacity-achieving NOMA transmission scheme, where users share the same time and frequency resources by invoking superposition coding at the AP and SIC at the users. Based on the NOMA principle, each user employs SIC to remove the intra-cell interference. The user with a stronger channel gain can decode the signal of the user with weaker channel gain. Let  $\mu_k(t)$  denote the decoding order for user  $k$  at time instant  $t$ . For instance, if  $\mu_k(t) = i$ , then user  $k$  is the  $i$ th signal to be decoded. For any two users  $j$  and  $k$  satisfying  $\mu_j(t) < \mu_k(t)$ , the combined channel gains of the two users need to satisfy  $|h_k + \mathbf{g}_k^H \Theta(t) \mathbf{v}|^2 \geq |h_j + \mathbf{g}_j^H \Theta(t) \mathbf{v}|^2$ . Therefore, the instantaneous achievable rate of user  $k$  in the NOMA scheme is given by

$$R_k^N(t) = \log_2 \left( 1 + \frac{|h_k + \mathbf{g}_k^H \Theta(t) \mathbf{v}|^2 p_k(t)}{\sum_{\mu_i(t) > \mu_k(t)} |h_k + \mathbf{g}_k^H \Theta(t) \mathbf{v}|^2 p_i(t) + \sigma^2} \right). \quad (3)$$

Similarly, the average achievable rate of user  $k$  over the entire period  $T$  in the NOMA scheme is  $\bar{R}_k^N = \frac{1}{T} \int_0^T R_k^N(t) dt$ .

## III. ERGODIC RATE AND CAPACITY REGIONS CHARACTERIZATION

The ergodic capacity region is defined as the set of all long-term average achievable rate over the time-varying channel, which can be achieved by the NOMA transmission (i.e., superposition coding and SIC) [31]. Though the AP-user channels are static during the coherence block duration  $T$ , the artificial time-varying channels can be established by dynamically adjusting the IRS phase-shift matrix. The ergodic capacity provides a good performance limit indicator for delay-insensitive applications. In the following, we characterize the ergodic rate and capacity regions<sup>2</sup> by jointly optimizing the IRS phase-shift matrix and resource allocations for both OMA and

<sup>2</sup>As the NOMA transmission scheme has been proved to be capacity-achieving in [31], we define the ergodic rate region and capacity region to be the set of average achievable rate-tuples for all users with OMA and NOMA, respectively. The similar definition is also applied for the delay-limited rate and capacity regions in Section IV.

NOMA transmission schemes.

#### A. OMA

We first study the ergodic rate region with the OMA transmission scheme. Let  $\mathcal{X}^O$  denote the feasible set of  $\{\Theta(t), p_k(t), \omega_k(t), \forall t\}$  specified by the discrete phase shift values, the maximum total transmit power constraint and the total orthogonal resources constraint. Then, the achievable ergodic rate region for OMA is defined as [31]

$$\mathcal{C}_{ergodic}^O \triangleq \bigcup_{\{\Theta(t), p_k(t), \omega_k(t)\} \in \mathcal{X}^O} \bar{\mathcal{C}}_{ave}^O(\{\Theta(t), p_k(t), \omega_k(t)\}), \quad (4)$$

where  $\bar{\mathcal{C}}_{ave}^O(\{\Theta(t), p_k(t), \omega_k(t)\}) = \{\bar{\mathbf{r}} : 0 \leq \bar{r}_k \leq \bar{R}_k^O, \forall k\}$  denotes the set of all achievable average rate-tuples  $\bar{\mathbf{r}} \triangleq (\bar{r}_1, \bar{r}_2, \dots, \bar{r}_K)$  for all  $K$  users under given  $\{\Theta(t), p_k(t), \omega_k(t), \forall t\}$ .

From the definition in (4),  $\mathcal{C}_{ergodic}^O$  consists of the set of average rate-tuples for all users that can be simultaneously achieved over the period  $T$  with the OMA transmission scheme. The upper-right boundary of this rate region is called the *Pareto boundary*, at which it is impossible to improve the rate of one user without simultaneously decreasing the rate of the other users. In order to characterize the complete Pareto boundary, we invoke the *rate-profile* technique [32], which is guaranteed to find all Pareto boundary points even if the region is a non-convex set. Specifically, let  $\boldsymbol{\alpha} = [\alpha_1, \alpha_2, \dots, \alpha_K]$  denote a rate-profile vector, where  $\alpha_k$  represents the rate allocation among the  $K$  users. We have  $\sum_{k=1}^K \alpha_k = 1$  and  $\alpha_k \geq 1, \forall k$ . Then, the characterization of any Pareto boundary point of the ergodic rate region for the OMA scheme is formulated as the following optimization problem

$$(P1) : \max_{R_{ave}^O, \bar{\mathbf{r}}, \{\Theta(t), p_k(t), \omega_k(t)\}} R_{ave}^O \quad (5a)$$

$$\text{s.t. } \bar{r}_k \geq \alpha_k R_{ave}^O, \forall k, \quad (5b)$$

$$\bar{\mathbf{r}} \in \bar{\mathcal{C}}_{ave}^O(\{\Theta(t), p_k(t), \omega_k(t)\}), \quad (5c)$$

$$\Theta(t) \in \mathcal{S}, \forall t, \quad (5d)$$

$$\sum_{k=1}^K p_k(t) \leq P_{max}, \forall t, \quad (5e)$$

$$\sum_{k=1}^K \omega_k(t) \leq 1, \forall t, \quad (5f)$$

$$p_k(t) \geq 0, 0 \leq \omega_k(t) \leq 1, \forall k, t, \quad (5g)$$

where  $R_{ave}^O$  denotes the average achievable sum rate of the  $K$  users in the OMA transmission scheme. Constraint (5d) represents the discrete phase-shift matrix constraint. Constraint (5e) and constraints (5f) are the total transmit power and orthogonal resources constraints.



Problems (P1) is a non-convex problems due to the non-convex set  $\mathcal{S}$  and the non-convex constraint (5c), where the optimization variables are highly coupled. Moreover, problem (P1) involves an infinite number of optimization variables. However, it can be shown that problem (P1) satisfies the time-sharing condition [29]. Therefore, the strong duality [33] holds and the duality gap between the primal problem and its Lagrange dual problem is zero. Hence, we can derive the optimal solution to (P1) via its dual problem.

Next, we invoke the Lagrange duality method to optimally solve (P1), the partial Lagrangian function of which is given by

$$\begin{aligned} \mathcal{L}_1 \left( R_{ave}^O, \Theta(t), \{p_k(t), \omega_k(t)\}, \{\lambda_k^{ave,O}\} \right) &= \left( 1 - \sum_{k=1}^K \alpha_k \lambda_k^{ave,O} \right) R_{ave}^O \\ &+ \sum_{k=1}^K \frac{\lambda_k^{ave,O}}{T} \int_0^T \omega_k(t) \log_2 \left( 1 + \frac{|h_k + \mathbf{g}_k^H \Theta(t) \mathbf{v}|^2 p_k(t)}{\omega_k(t) \sigma^2} \right) dt, \end{aligned} \quad (6)$$

where  $\{\lambda_k^{ave,O}\}$  are the non-negative Lagrange multipliers associated with constraint (5b). Accordingly, the Lagrange dual function of problem (P1) is given by

$$f_1 \left( \{\lambda_k^{ave,O}\} \right) = \max_{R_{ave}^O, \Theta(t), \{p_k(t), \omega_k(t)\}} \mathcal{L}_1 \left( R_{ave}^O, \Theta(t), \{p_k(t), \omega_k(t)\}, \{\lambda_k^{ave,O}\} \right) \quad (7a)$$

$$\text{s.t. (5d) - (5g).} \quad (7b)$$

**Lemma 1.** In order for the dual function  $f_1 \left( \{\lambda_k^{ave,O}\} \right)$  to be upper-bounded from above, i.e.,  $f_1 \left( \{\lambda_k^{ave,O}\} \right) < +\infty$ , it must hold that  $\sum_{k=1}^K \alpha_k \lambda_k = 1$ .

*Proof.* This is shown by contradiction. Suppose that  $\sum_{k=1}^K \alpha_k \lambda_k^{ave,O} > 1$  or  $\sum_{k=1}^K \alpha_k \lambda_k^{ave,O} < 1$ . Then, by setting  $R_{ave}^O \rightarrow -\infty$  or  $R_{ave}^O \rightarrow +\infty$ , we have  $f_1 \left( \{\lambda_k^{ave,O}\} \right) \rightarrow +\infty$ . Therefore, neither of the above two inequalities can be true and the lemma is proved.  $\square$

Based on **lemma 1**, the dual problem of problem (P1) is given by

$$(D1) : \min_{\{\lambda_k^{ave,O}\}} f_1 \left( \{\lambda_k^{ave,O}\} \right) \quad (8a)$$

$$\text{s.t. } \sum_{k=1}^K \alpha_k \lambda_k^{ave,O} = 1, \lambda_k^{ave,O} \geq 0, \forall k. \quad (8b)$$

As the strong duality holds, we can solve problem (P1) by solving its dual problem (D1). First, we solve problem (7) to obtain  $f_1 \left( \{\lambda_k^{ave,O}\} \right)$  under any given dual variables  $\{\lambda_k^{ave,O}\}$ . With the given dual variables, problem (7) can be decomposed into the following subproblems.

$$\max_{R_{ave}^O} \left( 1 - \sum_{k=1}^K \alpha_k \lambda_k^{ave,O} \right) R_{ave}^O \quad (9)$$

$$\max_{\{p_k(t), \omega_k(t)\}, \Theta(t)} \sum_{k=1}^K \varphi_k \left( \Theta(t), p_k(t), \omega_k(t), \lambda_k^{ave, O} \right), \forall t \quad (10a)$$

$$\text{s.t. (5d) - (5g),} \quad (10b)$$

where  $\varphi_k \left( \Theta(t), p_k(t), \omega_k(t), \lambda_k^{ave, O} \right) = \frac{\lambda_k^{ave, O}}{T} \omega_k(t) \log_2 \left( 1 + \frac{|h_k + \mathbf{g}_k^H \Theta(t) \mathbf{v}|^2 p_k(t)}{\omega_k(t) \sigma^2} \right)$ . Problem (10) consists of an infinite number of subproblems, each corresponding to one time instant  $t$ .

As  $\sum_{k=1}^K \alpha_k \lambda_k^{ave, O} = 1$ , the objective function value of subproblem (9) is always zero. In this case, we can choose any arbitrary real number as the optimal solution  $R_{ave}^{*O}$ . We set  $R_{ave}^{*O} = 0$  for simplicity. Therefore, we just need to focus on subproblem (10). Since the subproblems in (10) are identical for different time instants  $t$ 's, we can drop the index  $t$  for ease of exposition. We denote the optimal solutions to problem (10) as  $\Theta^*$ ,  $\{p_k^*\}$  and  $\{\omega_k^*\}$ . To solve problem (10), we have the following lemma.

**Lemma 2.** The optimal IRS phase-shift matrix, power allocation and orthogonal resource allocation to problem (10) are given by

$$\Theta^* = \Theta_{k^*}, p_k^* = \begin{cases} P_{\max}, & \text{if } k = k^* \\ 0, & \text{otherwise} \end{cases}, \omega_k^* = \begin{cases} 1, & \text{if } k = k^* \\ 0, & \text{otherwise} \end{cases}$$

where  $\Theta_k = \arg \max_{\Theta \in \mathcal{S}} |h_k + \mathbf{g}_k^H \Theta \mathbf{v}|^2, \forall k$  and  $k^* = \arg \max_{k \in \mathcal{K}} \frac{\lambda_k^{ave, O}}{T} \log_2 \left( 1 + \frac{|h_k + \mathbf{g}_k^H \Theta_k \mathbf{v}|^2 P_{\max}}{\sigma^2} \right)$ .

*Proof.* See Appendix A.  $\square$

It is worth noting that when using the Lagrange dual method to solve a convex problem via its dual problem, the optimal solution which maximizes the Lagrange function under the optimal dual solution is the optimal primal solution if and only if such a solution is unique and primal feasible [33]. In our case, the optimal solution  $R_{ave}^{*O}$  is non-unique since  $\sum_{k=1}^K \alpha_k \lambda_k^{ave, O} = 1$ . Additional steps are required to construct the optimal primal solution to problem (P1). Furthermore, **Lemma 2** reveals that there is only one user served according to the optimal solution to problem (10). With this insight, the total non-unique optimal solutions  $\Theta^*$ ,  $\{p_k^*\}$  and  $\{\omega_k^*\}$  to problem (10) can be directly obtained using the following proposition instead of truly finding the optimal dual solutions  $\{\lambda_k^{*ave, O}\}$ .

**Proposition 1.** For a given rate-profile vector  $\alpha$ , let  $\Upsilon$  denote the user index set with a non-zero rate target ratio,  $\Upsilon = \{k | \alpha_k > 0\}$ . Suppose that the optimal dual solutions are  $\{\lambda_k^{*ave, O}\}$  to (D1), then problem (10) has a total of  $|\Upsilon|$  optimal solutions  $\{\Gamma_k, k \in \Upsilon\}$  which are given by

$$\Gamma_k = \{\Theta_k, (\mathbf{0}_{k-1}, P_{\max}, \mathbf{0}_{K-k}), (\mathbf{0}_{k-1}, 1, \mathbf{0}_{K-k})\}, \quad (11)$$

where  $\Theta_k = \arg \max_{\Theta \in \mathcal{S}} |h_k + \mathbf{g}_k^H \Theta \mathbf{v}|^2$ ,  $k \in \Upsilon$  and it must hold that  $\varphi_k \left( \Gamma_k, \lambda_k^{*ave,O} \right) = \varphi_i \left( \Gamma_i, \lambda_i^{*ave,O} \right)$ ,  $k, i \in \Upsilon$  for problem (10).

*Proof.* This is shown by contradiction. Suppose that the  $k$ th term  $\varphi_k \left( \Gamma_k, \lambda_k^{*ave,O} \right)$  is smaller than any one of the other  $|\Upsilon| - 1$  terms (i.e.,  $\varphi_i \left( \Gamma_i, \lambda_i^{*ave,O} \right)$ ,  $\forall i \in \Upsilon, i \neq k$ ). In this case,  $\Gamma_k$  cannot be the optimal solution to problem (10). Then, the  $k$ th user cannot be served throughout the whole period  $T$ , which causes a zero rate for the  $k$ th user with a non-zero rate requirement. As a result, to achieve a non-zero rate, it must hold that  $\varphi_k \left( \Gamma_k, \lambda_k^{*ave,O} \right) = \varphi_i \left( \Gamma_i, \lambda_i^{*ave,O} \right)$ ,  $k, i \in \Upsilon$ , which contradicts our initial assumption and the proposition is proved.  $\square$

Based on **Proposition 1**, we need to determine the time-sharing ratio among the  $|\Upsilon|$  optimal solutions  $\{\Gamma_k, k \in \Upsilon\}$  to construct the optimal primal solution to problem (P1). Here, time-sharing means that the total  $K$  users should be served in an alternative manner for a certain portion of the total block duration  $T$ . Let  $\tau_k$  denote the optimal transmission duration for the  $k$ th user. Then, the optimal primal solution to (P1) can be obtained by solving the following problem

$$\max_{R_{sum}^{ave,O}, \{\tau_k \geq 0\}} R_{ave}^O \quad (12a)$$

$$\text{s.t. } \frac{\tau_k}{T} \log_2 \left( 1 + \frac{|h_k + \mathbf{g}_k^H \Theta_k \mathbf{v}|^2 P_{max}}{\sigma^2} \right) \geq \alpha_k R_{ave}^O, \forall k, \quad (12b)$$

$$\sum_{k=1}^{|\Upsilon|} \tau_k = T. \quad (12c)$$

It can be verified that the above problem is a standard linear program (LP), which can be solved by using standard convex optimization tools such as CVX [34]. Therefore, the optimal solution to (P1) with a given rate-profile vector  $\alpha$  can be obtained. The algorithm for optimally solving problem (P1) is summarized in Algorithm 1. The complexity of step 1) is  $\mathcal{O}(L^M |\Upsilon|)$  and of solving the LP problem (12) is  $\mathcal{O}(|\Pi|^3)$  [33]. The total complexity of Algorithm 1 is  $\mathcal{O}(L^M |\Upsilon| + |\Upsilon|^3)$ .

---

**Algorithm 1** Algorithm for Optimally Solving Problem (P1)

---

- 1: Find the total  $|\Upsilon|$  optimal solutions  $\{\Gamma_k, k \in \Upsilon\}$  with (11).
  - 2: Obtain the optimal solution  $R_{ave}^{*O}$  to problem (P1) via time-sharing by solving problem (12).
- 

**Remark 2.** The optimal solution to problem (12) implies that to achieve any point on the Pareto boundary of the ergodic rate region in the OMA scheme, the optimal transmission strategy follows the alternative transmission strategy where each user is alternatively served with its effective channel gain maximized by dynamically adjusting the IRS phase-shift matrix.

**Remark 3.** If the IRS is equipped with continuous phase shifts, the closed-form solution to  $\Theta_k = \arg \max_{\Theta \in \mathcal{S}} |h_k + \mathbf{g}_k^H \Theta \mathbf{v}|^2$  is  $\theta_m^{*k} = \arg(h_k) - \arg(g_{m,k}^H v_m)$ , where  $g_{m,k}^H$  and  $v_m$  are the  $m$ th element of  $\mathbf{g}_k^H$  and  $\mathbf{v}$ , respectively. This closed form solution follows intuitively from: 1) Triangle Inequality which says that the magnitude of the sum of 2 complex vectors is maximized when the 2 vectors are aligned (same direction). In this case:  $|\mathbf{x} + \mathbf{y}| = |\mathbf{x}| + |\mathbf{y}|$ . 2) Cauchy-Schwartz Inequality which says that the magnitude of the dot product is maximized when the two vectors are aligned. The ergodic rate region achieved with continuous phase shifts in OMA provides an upper bound to that with discrete phase shifts.

### B. NOMA

Next, we characterize the ergodic capacity region with the NOMA transmission scheme. Let  $\mathcal{X}^N$  denote the feasible sets of  $\{\Theta(t), p_k(t), \forall t\}$  specified by the discrete phase shift values and the maximum total transmit power constraint. Accordingly, the ergodic capacity region achieved by NOMA is defined as [31]

$$\mathcal{C}_{ergodic}^N \triangleq \bigcup_{\{\Theta(t), p_k(t)\} \in \mathcal{X}^N} \bar{\mathcal{C}}_{ave}^N(\{\Theta(t), p_k(t)\}), \quad (13)$$

where  $\bar{\mathcal{C}}_{ave}^N(\{\Theta(t), p_k(t)\}) = \{\bar{\mathbf{r}} : 0 \leq \bar{r}_k \leq \bar{R}_k^N, \forall k\}$ . In order to characterize the Pareto boundary of the ergodic capacity region  $\mathcal{C}_{ergodic}^N$ , we still invoke the rate-profile technique. Under the rate-profile vector  $\boldsymbol{\alpha} = [\alpha_1, \alpha_2, \dots, \alpha_K]$ , the Pareto boundary point of the capacity region  $\mathcal{C}_{ergodic}^N$  can be characterized by solving the following problem

$$(P2) : \max_{R_{ave}^N, \bar{\mathbf{r}}, \{\Theta(t), p_k(t)\}} R_{ave}^N \quad (14a)$$

$$\text{s.t. } \bar{r}_k \geq \alpha_k R_{ave}^N, \forall k, \quad (14b)$$

$$\bar{\mathbf{r}} \in \bar{\mathcal{C}}_{ave}^N(\{\Theta(t), p_k(t)\}), \quad (14c)$$

$$\Theta(t) \in \mathcal{S}, \forall t, \quad (14d)$$

$$\sum_{k=1}^K p_k(t) \leq P_{max}, \forall t, \quad (14e)$$

$$p_k(t) \geq 0, \forall k, t, \quad (14f)$$

$$|h_k + \mathbf{g}_k^H \Theta(t) \mathbf{v}|^2 \geq |h_j + \mathbf{g}_j^H \Theta(t) \mathbf{v}|^2, \text{ if } \mu_j(t) < \mu_k(t) \forall k, j, t, \quad (14g)$$

where  $R_{ave}^N$  denotes the average achievable sum rate of the  $K$  users in the NOMA transmission scheme. Constraint (14g) indicates the decoding order among users using the corresponding effective channel gain. Similarly, problem (P2) also satisfies the time-sharing condition and we still derive the optimal solution via its dual problem.

By utilizing the Lagrange duality method, the partial Lagrangian function of problem (P2) can be expressed as

$$\begin{aligned} \mathcal{L}_2 \left( R_{ave}^N, \Theta(t), \{p_k(t)\}, \{\lambda_k^{ave,N}\} \right) &= \left( 1 - \sum_{k=1}^K \alpha_k \lambda_k^{ave,N} \right) R_{sum}^{D-N} \\ &+ \sum_{k=1}^K \frac{\lambda_k^{ave,N}}{T} \int_0^T \log_2 \left( 1 + \frac{|h_k + \mathbf{g}_k^H \Theta(t) \mathbf{v}|^2 p_k(t)}{\sum_{\mu_i(t) > \mu_k(t)} |h_k + \mathbf{g}_k^H \Theta(t) \mathbf{v}|^2 p_i(t) + \sigma^2} \right) dt. \end{aligned} \quad (15)$$

where  $\{\lambda_k^{ave,N}\}$  are the non-negative Lagrange multipliers associated with constraint (14b).

Accordingly, the Lagrange dual function of problem (P2) is

$$f_2 \left( \{\lambda_k^{ave,N}\} \right) = \max_{R_{ave}^N, \Theta(t), \{p_k(t)\}} \mathcal{L}_2 \left( R_{ave}^N, \Theta(t), \{p_k(t)\}, \{\lambda_k^{ave,N}\} \right) \quad (16a)$$

$$\text{s.t. (14d) - (14g).} \quad (16b)$$

Similarly, the condition that  $\sum_{k=1}^K \alpha_k \lambda_k^{ave,N} = 1$  must be satisfied to ensure that  $f_2 \left( \{\lambda_k^{ave,N}\} \right)$  is bounded from above. Then, the dual problem of problem (P2) is

$$(D2) : \min_{\{\lambda_k^{ave,N}\}} f_2 \left( \{\lambda_k^{ave,N}\} \right) \quad (17a)$$

$$\text{s.t. } \sum_{k=1}^K \alpha_k \lambda_k^{ave,N} = 1, \lambda_k^{ave,N} \geq 0, \forall k. \quad (17b)$$

As the strong duality holds, we can optimally solve problem (P2) by solving its dual problem (D2). In the following, we first solve problem (16) to obtain  $f_2 \left( \{\lambda_k^{ave,N}\} \right)$  under any given dual variables, then solve problem (D2) to find the optimal dual variables  $\{\lambda_k^{*ave,N}\}$  to minimize  $f_2 \left( \{\lambda_k^{ave,N}\} \right)$ , and finally construct the optimal primal solution to problem (P2).

1) *Obtaining  $f_2 \left( \{\lambda_k^{ave,N}\} \right)$  by Solving Problem (16):* In order to obtain  $f_2 \left( \{\lambda_k^{ave,N}\} \right)$  for given dual variables  $\{\lambda_k^{ave,N}\}$ , we set  $R_{ave}^{*N} = 0$  and drop the time index  $t$ . Then, problem (16) can be expressed as

$$\max_{\Theta, \{p_k\}} \sum_{k=1}^K \frac{\lambda_k^{ave,N}}{T} \log_2 \left( 1 + \frac{|h_k + \mathbf{g}_k^H \Theta \mathbf{v}|^2 p_k}{\sum_{\mu_i > \mu_k} |h_k + \mathbf{g}_k^H \Theta \mathbf{v}|^2 p_i + \sigma^2} \right) \quad (18a)$$

$$\text{s.t. } \Theta \in \mathcal{S}, \quad (18b)$$

$$\sum_{k=1}^K p_k \leq P_{max}, p_k \geq 0, \forall k, \quad (18c)$$

$$|h_k + \mathbf{g}_k^H \Theta \mathbf{v}|^2 \geq |h_j + \mathbf{g}_j^H \Theta \mathbf{v}|^2, \text{ if } \mu_j < \mu_k. \quad (18d)$$

Problem (18) can be regarded as a weighted sum rate maximization problem. The optimal solution is achieved when (18c) is satisfied with equality, since otherwise we can always increase the

power allocation to the strongest user  $p_K$  to increase the cost function. For ease of exposition, we assume that the decoding order is  $\mu_k \triangleq k, \forall k$  and define  $q_k = \sum_{i=k}^K p_i, \forall k$ , where  $q_1 = P_{max}$ .

The  $k$ th term in (18a) can be expressed as

$$\begin{aligned} & \log_2 \left( 1 + \frac{|h_k + \mathbf{g}_k^H \Theta \mathbf{v}|^2 p_k}{\sum_{i>k} |h_k + \mathbf{g}_k^H \Theta \mathbf{v}|^2 p_i + \sigma^2} \right) \\ & = \log_2 \left( \sigma^2 + |h_k + \mathbf{g}_k^H \Theta \mathbf{v}|^2 q_k \right) - \log_2 \left( \sigma^2 + |h_k + \mathbf{g}_k^H \Theta \mathbf{v}|^2 q_{k+1} \right). \end{aligned} \quad (19)$$

Next, we first focus on the weighted sum rate maximization problem under any given dual variables  $\{\lambda_k^{ave,N}\}$  and IRS phase-shift matrix  $\Theta$ . Let  $\phi(\{\lambda_k^{ave,N}\}, \Theta)(\{q_k\})$  denote the corresponding objective function, the optimization problem can be expressed as

$$\max_{\{q_k\}} \phi(\{\lambda_k^{ave,N}\}, \Theta)(\{q_k\}) \quad (20a)$$

$$\text{s.t. } P_{max} = q_1 \geq q_2 \geq \dots \geq q_K \geq 0, \quad (20b)$$

where

$$\begin{aligned} \phi(\{\lambda_k^{ave,N}\}, \Theta)(\{q_k\}) &= \frac{\lambda_1^{ave,N}}{T} \log_2 \left( \sigma^2 + |h_1 + \mathbf{g}_1^H \Theta \mathbf{v}|^2 q_1 \right) - \frac{\lambda_K^{ave,N}}{T} \log_2 \left( \sigma^2 \right) \\ &+ \sum_{k=2}^K \left( \frac{\lambda_k^{ave,N}}{T} \log_2 \left( \sigma^2 + |h_k + \mathbf{g}_k^H \Theta \mathbf{v}|^2 q_k \right) - \frac{\lambda_{k-1}^{ave,N}}{T} \log_2 \left( \sigma^2 + |h_{k-1} + \mathbf{g}_{k-1}^H \Theta \mathbf{v}|^2 q_k \right) \right). \end{aligned}$$

Since  $\phi(\{\lambda_k^{ave,N}\}, \Theta)(\{q_k\})$  is a continuous function over the feasible region  $\Psi = \{q_k, \forall k | P_{max} = q_1 \geq q_2 \geq \dots \geq q_K \geq 0\}$ , its maximum point is either at the stationary point or on the boundary of  $\Psi$ . To solve problem (20), we have the following lemma.

**Lemma 3.** For the  $K$  user case, the number of candidate solutions for achieving the maximum of  $\phi(\{\lambda_k^{ave,N}\}, \Theta)(\{q_k\})$  is  $2^K - 1$ .

*Proof.* The inequality sign in the constraint (20b) can be further decomposed into equality and strict inequality. As a result, the original constraint  $P_{max} = q_1 \underbrace{\geq}_1 q_2 \underbrace{\geq}_2 \dots \underbrace{\geq}_{K-1} q_K \underbrace{\geq}_K 0$  can be replaced with  $2^{K-1}$  independent constraints since it is infeasible for the case  $P_{max} = q_1 = q_2 = \dots = q_K = 0$ . Therefore, there are  $2^K - 1$  candidate solutions associated with each decomposed constraint to achieve the maximum of  $\phi(\{\lambda_k^{ave,N}\}, \Theta)(\{q_k\})$ . The proof is completed.  $\square$

**Lemma 3** provides important insights on how to maximize  $\phi(\{\lambda_k^{ave,N}\}, \Theta)(\{q_k\})$  based on the constraint (20b). From the definition of  $q_k$ , if  $q_k = q_{k+1}$ , it follows that the  $k$ th user is not served (i.e.,  $p_k = 0$ ); otherwise the  $k$ th user is served with  $p_k > 0$ . On this basis, we derive the optimal solution of the two user and three user cases using the following proposition.

**Proposition 2.** The optimal power allocation to problem (20) with two users is given by

$$(q_1^*, q_2^*) = \arg \max \left\{ \phi(\{\lambda_k^{ave,N}\}, \Theta) (P_{max}, 0), \phi(\{\lambda_k^{ave,N}\}, \Theta) (P_{max}, P_{max}), \phi(\{\lambda_k^{ave,N}\}, \Theta) (P_{max}, \bar{q}_2) \right\}$$

(21)

and with three users is given by

$$(q_1^*, q_2^*, q_3^*) = \arg \max \left\{ \phi(\{\lambda_k^{ave,N}\}, \Theta) (P_{max}, 0, 0), \phi(\{\lambda_k^{ave,N}\}, \Theta) (P_{max}, P_{max}, 0), \right. \\ \left. \phi(\{\lambda_k^{ave,N}\}, \Theta) (P_{max}, P_{max}, P_{max}), \phi(\{\lambda_k^{ave,N}\}, \Theta) (P_{max}, P_{max}, \bar{q}_3), \phi(\{\lambda_k^{ave,N}\}, \Theta) (P_{max}, \bar{q}_2, 0), \right. \\ \left. \phi(\{\lambda_k^{ave,N}\}, \Theta) (P_{max}, \bar{q}_3, \bar{q}_3), \phi(\{\lambda_k^{ave,N}\}, \Theta) (P_{max}, \bar{q}_2, \bar{q}_3) \right\},$$

where

$$\bar{q}_k = \left[ \frac{\left( \frac{\lambda_{k-1}^{ave,N}}{|h_k + \mathbf{g}_k^H \Theta \mathbf{v}|^2} - \frac{\lambda_k^{ave,N}}{|h_{k-1} + \mathbf{g}_{k-1}^H \Theta \mathbf{v}|^2} \right)}{\lambda_k^{ave,N} - \lambda_{k-1}^{ave,N}} \right]_0^{P_{max}}, \forall k. \quad (22)$$

*Proof.* See Appendix B. □

Therefore, we can optimally solve problem (20) by checking all candidate solutions. Based on problem (20), we adopt exhaustive search over the IRS phase-shift matrix set  $\mathcal{S}$  to obtain the optimal IRS phase-shift matrix to problem (18) under given  $\{\lambda_k^{ave,N}\}$  as

$$\Theta^* = \arg \max_{\Theta \in \mathcal{S}} \left\{ \max_{\{q_k\}} \phi(\{\lambda_k^{ave,N}\}, \Theta) (\{q_k\}) \right\}. \quad (24)$$

Accordingly, the optimal power allocation solutions to problem (18) under given  $\{\lambda_k^{ave,N}\}$  are given by

$$p_k^* = q_k^*(\{\lambda_k^{ave,N}\}, \Theta^*) - q_{k+1}^*(\{\lambda_k^{ave,N}\}, \Theta^*), 1 \leq k \leq K-1, \\ p_K^* = q_K^*(\{\lambda_k^{ave,N}\}, \Theta^*). \quad (25)$$

By substituting the above optimal solutions  $\{\Theta^*, \{p_k^*\}\}$  into problem (16), the dual function  $f_2(\{\lambda_k^{ave,N}\})$  is obtained.

2) *Finding Optimal Dual Solution to (D2):* Next, we search over  $\{\lambda_k^{ave,N}\}$  to minimize  $f(\{\lambda_k^{ave,N}\})$  for solving (D2). Since the dual problem (D2) is always convex but in general non-differentiable, the subgradient-based methods such as the ellipsoid method [35] can be used to solve problem (D2). Note that the subgradient of the objective function  $f_2(\{\lambda_k^{ave,N}\})$  is denoted by  $s_0 = \Delta \lambda$ , where  $\Delta \lambda_k = \log_2 \left( 1 + \frac{|h_k + \mathbf{g}_k^H \Theta^* \mathbf{v}|^2 p_k^*}{\sum_{\mu_i > \mu_k} |h_k + \mathbf{g}_k^H \Theta^* \mathbf{v}|^2 p_i^* + \sigma^2} \right)$ ,  $\forall k$ . Moreover, the equality constraint (17b) is equivalent to the two inequality constraints:  $1 - \sum_{k=1}^K \alpha_k \lambda_k \leq 0$  and  $-1 + \sum_{k=1}^K \alpha_k \lambda_k \leq 0$ , whose subgradients are given by  $s_1 = -\alpha$  and  $s_2 = -s_1$ . With the above

subgradients, the dual variables can be updated by the constrained ellipsoid method. The optimal dual solutions to (D2) are denoted by  $\{\lambda_k^{*ave,N}\}$ .

3) *Constructing Optimal Primal Solution to Problem (P2)*: With the obtained optimal dual variable  $\{\lambda_k^{*ave,N}\}$  using the constrained ellipsoid method, we need to find the optimal primal solutions to problem (P2). Since the optimal solutions  $\Theta^*$ ,  $\{p_k^*\}$  and  $R_{ave}^{*N}$  to problem (16) with  $\{\lambda_k^{*ave,N}\}$  are generally non-unique, additional steps are required to construct the optimal primal solution by deciding the time-sharing ratio among all optimal solutions. Suppose that problem (16) under  $\{\lambda_k^{*ave,N}\}$  has a total number of  $\Pi$  optimal solutions, denoted by  $\{(\Theta^\varpi, \{p_k^\varpi\})\}_{\varpi=1}^\Pi$ . Let  $\tau_\varpi$  denote the optimal transmission duration at the  $\varpi$ th optimal solution. Then, the optimal primal solution to (P2) can be obtained by solving the following problem

$$\max_{R_{ave}^N, \{\tau_\varpi \geq 0\}} R_{ave}^N \quad (26a)$$

$$\text{s.t.} \quad \sum_{\varpi=1}^\Pi \frac{\tau_\varpi}{T} \log_2 \left( 1 + \frac{|h_k + \mathbf{g}_k^H \Theta_\varpi \mathbf{v}|^2 p_k^\varpi}{\sum_{\mu_i^\varpi > \mu_k^\varpi} |h_k + \mathbf{g}_k^H \Theta_\varpi \mathbf{v}|^2 p_i^\varpi + \sigma^2} \right) \geq \alpha_k R_{ave}^N, \forall k, \quad (26b)$$

$$\sum_{\varpi=1}^\Pi \tau_\varpi = T. \quad (26c)$$

Similarly, problem (26) is a standard LP, which can be solved by using standard convex optimization tools such as CVX [34]. As a result, the optimal solution to problem (P2) is obtained.

The details of the procedures for optimally solving problem (P2) are summarized in **Algorithm 2**.

The computational complexity of Algorithm 2 is dominated by the ellipsoid method in steps 1)-4) and solving the LP problem (26). Specifically, the complexity of steps 2)-3) is  $\mathcal{O}(L^M K^2)$ .

As the ellipsoid method requires  $\mathcal{O}\left(\frac{K^2}{\varepsilon}\right)$  to converge [35], the total complexity for steps 1)-4) is  $\mathcal{O}\left(\frac{L^M K^4}{\varepsilon}\right)$ . The complexity of solving problem (26) is  $\mathcal{O}(|\Pi|^3)$ . Therefore, the total complexity for optimally solving (P2) is  $\mathcal{O}\left(\frac{L^M K^4}{\varepsilon} + |\Pi|^3\right)$ .

**Remark 4.** The optimal solution to (P2) for achieving the Pareto boundary of the capacity region shares the same philosophy as that of (P1). However, in the NOMA scheme, the optimal strategy follows alternative transmission among different user groups or decoding orders with properly designed IRS phase-shift matrix.

#### IV. DELAY-LIMITED RATE AND CAPACITY REGIONS CHARACTERIZATION

Delay-limited capacity (also referred to as the zero-outage capacity) is defined as the set of all instantaneous achievable rate that can be always maintained over the time-varying channel [36].

Compared with the ergodic capacity, delay-limited capacity is more suitable for characterizing



---

**Algorithm 2** Algorithm for Optimally Solving Problem (P2)
 

---

Initialize an ellipsoid  $\mathcal{E} \left( \left\{ \lambda_k^{ave,N} \right\}, \mathbf{A} \right)$  containing  $\left\{ \lambda_k^{*ave,N} \right\}$ , where  $\left\{ \lambda_k^{ave,N} \right\}$  is the center point of  $\mathcal{E}$  and the positive definite matrix  $\mathbf{A}$  characterizes the size of  $\mathcal{E}$ .

1: **repeat**

2: Obtain  $R_{ave}^{*N}, \Theta^*, \{p_k^*\}$  based on (24) and (25).

3: Update  $\left\{ \lambda_k^{ave,N} \right\}$  using the constrained ellipsoid with the corresponding subgradients.

4: **until**  $\left\{ \lambda_k^{ave,N} \right\}$  converge with a prescribed accuracy.

5: **Set**  $\left\{ \lambda_k^{*ave,N} \right\} \leftarrow \left\{ \lambda_k^{ave,N} \right\}$ .

6: Obtain  $\left\{ (\Theta^\varpi, \{p_k^\varpi\}) \right\}_{\varpi=1}^\Pi$  by solving problem (18) under  $\left\{ \lambda_k^{*ave,N} \right\}$ .

7: Construct the optimal solution  $R_{ins}^{*ave,N}$  to problem (P2) via time-sharing by solving problem (26).

---

the performance limit of real-time applications such as video streaming, which requires a constant rate during the whole service. In the following, we characterize the delay-limited rate and capacity regions by jointly optimizing the IRS phase-shift matrix and resource allocations for both OMA and NOMA transmission schemes.

#### A. OMA

Since the delay-limited capacity is concerned with the instantaneous achievable rate of users, the achievable delay-limited rate region for OMA is defined as [36]

$$\mathcal{C}_{zero}^O \triangleq \bigcup_{\{\Theta(t), p_k(t), \omega_k(t)\} \in \mathcal{X}^O} \bar{\mathcal{C}}_{ins}^O(\{\Theta(t), p_k(t), \omega_k(t)\}), \quad (27)$$

where  $\bar{\mathcal{C}}_{ins}^O(\{\Theta(t), p_k(t), \omega_k(t)\}) = \{\mathbf{r} : 0 \leq r_k \leq R_k^O, \forall k\}$  denotes the set of all achievable instantaneous rate-tuples  $\mathbf{r} \triangleq (r_1, r_2, \dots, r_K)$  for all  $K$  users under given  $\{\Theta(t), p_k(t), \omega_k(t), \forall t\}$ .

Similarly, by invoking the rate-profile technique, the Pareto boundary point of the delay-limited rate region  $\mathcal{C}_{zero}^O$  can be characterized by solving the following problem

$$(P3) : \max_{R_{ins}^O, \mathbf{r}, \{\Theta(t), p_k(t), \omega_k(t)\}} R_{ins}^O \quad (28a)$$

$$\text{s.t. } r_k \geq \alpha_k R_{ins}^O, \forall k, \quad (28b)$$

$$\mathbf{r} \in \bar{\mathcal{C}}_{ins}^O(\{\Theta(t), p_k(t), \omega_k(t)\}), \quad (28c)$$

$$(5d) - (5g). \quad (28d)$$

where  $R_{ins}^O$  denotes the instantaneous achievable sum rate of the  $K$  users in the OMA transmission scheme. Since problem (P3) is identical for all time instant  $t$ , we can drop the time index  $t$  for the ease of exposition. However, problem (P3) is still a non-convex problem due to the non-convex set  $\mathcal{S}$ . To address this issue, the optimal solution to (P3) can be obtained by exhaustively searching over all possible phase-shift matrices, i.e.,  $R_{ins}^{*O}(\boldsymbol{\alpha}) = \arg \max_{\Theta \in \mathcal{S}} R_{ins}^{*O}(\boldsymbol{\alpha}, \Theta)$ , where  $R_{ins}^{*O}(\boldsymbol{\alpha}, \Theta)$  denotes the optimal solution for the subproblem under a given IRS phase-shift matrix

$\Theta$ . In the following, we optimally solve the subproblem of problem (P3).

Under a given  $\Theta$ , problem (P3) can be written as

$$(P3\text{-sub}) : \max_{R_{ins}^O, \{p_k, \omega_k\}} R_{ins}^O \quad (29a)$$

$$\text{s.t. } \omega_k \log_2 \left( 1 + \frac{|h_k + \mathbf{g}_k^H \Theta \mathbf{v}|^2 p_k}{\omega_k \sigma^2} \right) \geq \alpha_k R_{ins}^O, \forall k, \quad (29b)$$

$$\sum_{k=1}^K p_k \leq P_{max}, \quad (29c)$$

$$\sum_{k=1}^K \omega_k \leq 1, \quad (29d)$$

$$p_k \geq 0, 0 \leq \omega_k \leq 1, \forall k, \quad (29e)$$

Define  $\omega_k \log_2 \left( 1 + \frac{|h_k + \mathbf{g}_k^H \Theta \mathbf{v}|^2 p_k}{\omega_k \sigma^2} \right) \triangleq 0$  when  $\omega_k = 0, \forall k$ , such that the left-hand-side (LHS) of (29b) is jointly concave with respect to  $\omega_k$  and  $p_k$ . Therefore, problem (P3-sub) is a convex problem. It can be verified that the Slater's constraint qualification is satisfied for problem (P3-sub) [33]. Hence, strong duality [33] holds and the duality gap between problem (P3-sub) and its Lagrange dual problem is zero. Then, we invoke the Lagrangian dual method to optimally solve problem (P3-sub). The partial Lagrange of problem (P3-sub) is given by

$$\begin{aligned} \mathcal{L}_3 (R_{ins}^O, \{p_k\}, \{\omega_k\}, \{\lambda_k\}, \delta, \nu) &= \left( 1 - \sum_{k=1}^K \alpha_k \lambda_k \right) R_{ins}^O \\ &+ \sum_{k=1}^K \lambda_k \omega_k \log_2 \left( 1 + \frac{|h_k + \mathbf{g}_k^H \Theta \mathbf{v}|^2 p_k}{\omega_k \sigma^2} \right) + \delta P_{max} - \delta \sum_{k=1}^K p_k + \nu - \nu \sum_{k=1}^K \omega_k, \end{aligned} \quad (30)$$

where  $\{\lambda_k\}$ ,  $\delta$  and  $\nu$  are the non-negative Lagrange multipliers associated with constraints (29b), (29c) and (29d), respectively. Then, the Lagrange dual function of problem (P3-sub) is

$$f_3 (\{\lambda_k\}, \delta, \nu) = \max_{R_{ins}^O, \{p_k\}, \{\omega_k\}} \mathcal{L}_3 (R_{ins}^O, \{p_k\}, \{\omega_k\}, \{\lambda_k\}, \delta, \nu) \quad (31a)$$

$$\text{s.t. } (29e). \quad (31b)$$

Similarly, the condition that  $\sum_{k=1}^K \alpha_k \lambda_k = 1$  must be satisfied to ensure that  $f_3 (\{\lambda_k\}, \delta, \nu)$  is bounded from above. Then, the dual problem of problem (P3-sub) is given by

$$(D3) : \min_{\{\lambda_k\}, \nu, \delta} f_3 (\{\lambda_k\}, \delta, \nu) \quad (32a)$$

$$\text{s.t. } \sum_{k=1}^K \alpha_k \lambda_k = 1, \lambda_k \geq 0, \delta \geq 0, \nu \geq 0, \forall k. \quad (32b)$$

In order to obtain  $f_3 (\{\lambda_k\}, \delta, \nu)$  for given dual variables, we similarly set  $R_{ins}^{*O} = 0$ . Then, problem (32a) can be decomposed into the following  $K$  independent subproblems.

$$\max_{\omega_k, p_k} \lambda_k \omega_k \log_2 \left( 1 + \frac{|h_k + \mathbf{g}_k^H \Theta \mathbf{v}|^2 p_k}{\omega_k \sigma^2} \right) - \delta p_k - \nu \omega_k \quad \forall k \quad (33a)$$

$$\text{s.t. (29e).} \quad (33b)$$

The optimal solutions to each subproblem in (33) can be obtained using the following lemma.

**Lemma 4.** For the  $k$ th subproblem in (33), the optimal solutions are given by:

$$p_k^* = \omega_k^* t_k^*, \quad \forall k \quad (34)$$

and

$$\omega_k^* = \begin{cases} 0, & \text{if } h(t_k^*) < 0, \\ \omega \in [0, 1], & \text{if } h(t_k^*) = 0, \\ 1, & \text{otherwise, } \forall k, \end{cases} \quad (35)$$

where  $t_k^* = \left( \frac{\lambda_k}{\delta \ln 2} - \frac{\sigma^2}{|h_k + \mathbf{g}_k^H \Theta \mathbf{v}|^2} \right)^+$ ,  $(x)^+ \triangleq \max(x, 0)$  and  $h(t_k^*) = \lambda_k \log_2 \left( 1 + \frac{|h_k + \mathbf{g}_k^H \Theta \mathbf{v}|^2 t_k^*}{\sigma^2} \right) - \delta t_k^* - \nu$ .

*Proof.* Note that the subproblem (33) is jointly concave with respect to  $\omega_k$  and  $p_k$ , the KKT conditions are necessary and sufficient for the optimality of (33). First, by taking the derivative of the objective function of (33) with respect to  $p_k$ , the optimal power allocation  $p_k^*$  is obtained as (34). Next, by substituting  $p_k^* = \omega_k^* t_k^*$  into (33), we have the following problem

$$\max_{\omega_k} h(t_k^*) \omega_k \quad (36a)$$

$$\text{s.t. } 0 \leq \omega_k \leq 1. \quad (36b)$$

Note that problem (36) is a LP with respect to  $\omega_k$ . Specifically, when  $h(t_k^*) = 0$ , the optimal  $\omega_k^*$  can be set as any arbitrary real number  $\omega$  between 0 and 1. For simplicity, we set  $\omega = 0$ . Therefore, the optimal  $\omega_k^*$  is obtained as (35). The proof is completed.  $\square$

By substituting  $R_{ins}^{*O}$ ,  $\{p_k^*\}$  and  $\{\omega_k^*\}$  into problem (31), the dual function  $f_3(\{\lambda_k\}, \delta, \nu)$  is obtained. Next, with the obtained  $f_3(\{\lambda_k\}, \delta, \nu)$ , we can also find the optimal dual variables with the constrained ellipsoid method, the details of which are omitted. With the obtained optimal dual solutions  $\{\lambda_k^*\}, \delta^*$  and  $\nu^*$ , we need to find the optimal primal solutions  $\{p_k^*\}, \{\omega_k^*\}$  and  $R_{ins}^{*O}$  to problem (P3-sub). However, the optimal solutions to problem (31) are non-unique since  $\sum_{k=1}^K \alpha_k \lambda_k = 1$  and when  $h(t_k^*) = 0$  as in (35). As a result, additional steps are required to find the optimal primal solution. It is worth noting that with the given  $\{\lambda_k^*\}, \delta^*$  and  $\nu^*$ , variables  $\{t_k^*\}$  can be uniquely determined in **Lemma 4**. By substituting  $\{t_k^*\}$  into the primal problem (P3-sub), the optimization problem can be rewritten as

$$\max_{R_{ins}^O, \{\omega_k\}} R_{ins}^O \quad (37a)$$

---

**Algorithm 3** Algorithm for Optimally Solving Problem (P3-sub) under a given  $\Theta$ 


---

Initialize an ellipsoid  $\mathcal{E}(\{\lambda_k\}, \delta, \nu, \mathbf{A})$  containing  $(\{\lambda_k^*\}, \delta^*, \nu^*)$ , where  $(\{\lambda_k\}, \delta, \nu)$  is the center point of  $\mathcal{E}$  and the positive definite matrix  $\mathbf{A}$  characterizes the size of  $\mathcal{E}$ .

- 1: **repeat**
  - 2: Obtain  $R_{ins}^{*O}, \{p_k^*\}, \{\omega_k^*\}$  by solving problem (33).
  - 3: Update  $(\{\lambda_k\}, \delta, \nu)$  using the constrained ellipsoid with the corresponding subgradients.
  - 4: **until**  $(\{\lambda_k\}, \delta, \nu)$  converge with a prescribed accuracy  $\varepsilon$ .
  - 5: Set  $(\{\lambda_k^*\}, \delta^*, \nu^*) \leftarrow (\{\lambda_k\}, \delta, \nu)$ .
  - 6: Construct the optimal primal solutions to problem (P3-sub) by solving problem (37).
- 

$$\text{s.t. } \omega_k \log_2 \left( 1 + \frac{|h_k + \mathbf{g}_k^H \Theta \mathbf{v}|^2 t_k^*}{\sigma^2} \right) \geq \alpha_k R_{ins}^O, \forall k, \quad (37b)$$

$$\sum_{k=1}^K \omega_k t_k^* \leq P_{max}, \quad (37c)$$

$$\sum_{k=1}^K \omega_k \leq 1, 0 \leq \omega_k \leq 1, \forall k. \quad (37d)$$

Under given  $\{t_k^*\}$ , the above problem is a standard LP with respect to  $R_{ins}^O$  and  $\{\omega_k\}$ , which can be efficiently solved by using standard convex optimization tools such as CVX [34]. With the obtained optimal orthogonal resource allocation variables  $\{\omega_k^*\}$ , the corresponding power allocation can be obtained as  $p_k^* = \omega_k^* t_k^*, \forall k$ . The overall algorithm for optimally solving problem (P3-sub) for a given phase-shift matrix  $\Theta$  and rate-profile vector  $\alpha$  is summarized in **Algorithm 3**. Since the complexity of steps 2)-3) is  $\mathcal{O}(K^2)$ , the total complexity of the ellipsoid method in Algorithm 3 is  $\mathcal{O}\left(\frac{K^4}{\varepsilon}\right)$ . The complexity of solving problem (37) is  $\mathcal{O}(K^3)$ . Then, the complexity of Algorithm 3 is  $\mathcal{O}\left(\frac{K^4}{\varepsilon} + K^3\right)$ . Furthermore, in order to solve problem (P3), an exhaustive search over the IRS phase-shift matrix set  $\mathcal{S}$  is performed with the complexity of  $\mathcal{O}(L^M)$ . Therefore, the overall complexity for optimally solving (P3) is  $\mathcal{O}\left(L^M \left(\frac{K^4}{\varepsilon} + K^3\right)\right)$ .

### B. NOMA

Similarly, the delay-limited capacity region for NOMA is defined as [36]

$$\mathcal{C}_{zero}^N \triangleq \bigcup_{\{\Theta(t), p_k(t)\} \in \mathcal{X}^N} \bar{\mathcal{C}}_{ins}^N(\{\Theta(t), p_k(t)\}), \quad (38)$$

where  $\bar{\mathcal{C}}_{ins}^N(\{\Theta(t), p_k(t)\}) = \{\mathbf{r} : 0 \leq r_k \leq R_k^N, \forall k\}$ . With the rate-profile technique, the Pareto boundary characterization problem of the delay-limited capacity region  $\mathcal{C}_{zero}^N$  is formulated as

$$(P4) : \max_{R_{ins}^N, \mathbf{r}, \{\Theta(t), p_k(t)\}} R_{ins}^N \quad (39a)$$

$$\text{s.t. } r_k \geq \alpha_k R_{ins}^N, \forall k, \quad (39b)$$

$$\mathbf{r} \in \bar{\mathcal{C}}_{ins}^N(\{\Theta(t), p_k(t)\}), \quad (39c)$$

$$(14d) - (14g). \quad (39d)$$

Similarly, we can optimally solve problem (P4) by exhaustively searching over all possible phase-shift matrices  $\mathcal{S}$ , i.e.,  $R_{ins}^{**N}(\boldsymbol{\alpha}) = \arg \max_{\Theta \in \mathcal{S}} R_{ins}^{*N}(\boldsymbol{\alpha}, \Theta)$ , where  $R_{ins}^{*N}(\boldsymbol{\alpha}, \Theta)$  denotes the optimal solution for the problem (P4) under a given IRS phase-shift matrix  $\Theta$ . By dropping the time index  $t$ , the problem (P4) with a given IRS phase-shift matrix  $\Theta$  is expressed as

$$(P4\text{-sub}) : \max_{R_{ins}^N, \{p_k\}} R_{ins}^N \quad (40a)$$

$$\text{s.t. } \log_2 \left( 1 + \frac{|h_k + \mathbf{g}_k^H \Theta \mathbf{v}|^2 p_k}{\sum_{\mu_i > \mu_k} |h_k + \mathbf{g}_k^H \Theta \mathbf{v}|^2 p_i + \sigma^2} \right) \geq \alpha_k R_{ins}^N, \forall k, \quad (40b)$$

$$\sum_{k=1}^K p_k \leq P_{max}, \quad (40c)$$

$$p_k \geq 0, \forall k. \quad (40d)$$

where  $R_{ins}^N$  denotes the instantaneous achievable sum rate of the  $K$  users in the NOMA transmission scheme. It is worth noting that the decoding order among users is determined by the effective channel gains  $|h_k + \mathbf{g}_k^H \Theta \mathbf{v}|^2$ . Therefore, the decoding order in problem (P4-sub) is fixed under given  $\Theta$ . Though problem (P4-sub) is a non-convex problem due to the non-convex constraint (40b), we show that problem (P4-sub) is solvable by successively checking the feasibility under a given rate target  $r_{ins}^N$ . First, the non-convex constraint (40b) can be rearranged as

$$|h_k + \mathbf{g}_k^H \Theta \mathbf{v}|^2 p_k \geq \left( 2^{\alpha_k r_{ins}^N} - 1 \right) \left( \sum_{\mu_i > \mu_k} |h_k + \mathbf{g}_k^H \Theta \mathbf{v}|^2 p_i + \sigma^2 \right), \quad (41)$$

which is equivalent to (40b). Then, the feasibility of optimization problem (P4-sub) with fixed  $r_{ins}^N$  can be checked by solving the following problem

$$P^C = \min_{\{p_k\}} \sum_{k=1}^K p_k \quad (42a)$$

$$\text{s.t. } (40c), (40d), (41). \quad (42b)$$

It can be verified that problem (42) is a convex problem, which can be solved directly via a standard optimization tool such as CVX [34]. For a given sum rate target  $r_{ins}^N$ , if problem (42) is infeasible or the optimal value  $P^C > P_{max}$ , it follows that  $R_{ins}^{*N} < r_{ins}^N$ ; otherwise,  $R_{ins}^{*N} \geq r_{ins}^N$ . Therefore, by solving problem (42) with different  $r_{ins}^N$ 's with the bisection method, we can obtain the optimal solution  $R_{ins}^{*N}$  to problem (P4-sub). The overall algorithm for optimally solving problem (P4-sub) under a given phase-shift matrix  $\Theta$  and rate-profile vector  $\boldsymbol{\alpha}$  is summarized in **Algorithm 4**. The complexity of solving problem (42) is  $\mathcal{O}(K^3)$ . Then, the complexity of

---

**Algorithm 4** Algorithm for Optimally Solving Problem (P4-sub) under a given  $\Theta$ 


---

Given  $r_{max}$  and  $r_{min}$ .

- 1: **while**  $r_{max} - r_{min} \geq \varepsilon$ , **do**
  - 2: Check the feasibility of problem (42) with given  $r_{ins}^N = \frac{r_{max} + r_{min}}{2}$ .
  - 3: **if** problem (42) is feasible, **then**
  - 4:  $r_{min} = r_{ins}^N$ ,
  - 5: **else**
  - 6:  $r_{max} = r_{ins}^N$ ,
  - 7: **end if**
  - 8: **end while**
  - 9: Obtain the optimal solution  $R_{ins}^{*N} = r_{min}$  to problem (P4-sub).
- 

Algorithm 4 through the bisection method is  $\mathcal{O}(K^3 \log_2(\frac{\bar{r}_{max}}{\varepsilon}))$ , where  $\bar{r}_{max}$  is the initial upper bound. As a result, the overall complexity for optimally solving problem (P4) via exhaust search on  $\mathcal{S}$  is  $\mathcal{O}(L^M K^3 \log_2(\frac{\bar{r}_{max}}{\varepsilon}))$ .

**Remark 5.** In contrast with achieving the ergodic capacity by time-sharing among multiple non-unique optimal solutions, the optimal solutions to problems (P3) and (P4) are unique. For instance, the optimal IRS phase-shift matrix and the corresponding power allocation in the NOMA transmission can be uniquely determined by  $\{\Theta^*, \{p_k^*\}\} = \arg \max_{\Theta \in \mathcal{S}} \left\{ \max_{\{p_k\}} R_{ins}^O(\{p_k\}) \right\}$ . It indicates that the IRS phase-shift matrix should be fixed for achieving the Pareto boundary of the delay-limited rate and capacity regions.

**Remark 6.** As described in Section III and Section IV, an exhaustive search over all possible phase-shift matrices is required for optimally solving problems (P1)-(P4) with a complexity order of  $\mathcal{O}(L^M)$ . However, it may be unaffordable even for moderate  $M$ . To address this issue, we propose a codebook based scheme with the Hadamard matrix [37] to obtain a low-complexity suboptimal solution. A Hadamard matrix is an orthogonal matrix whose entries are either 1 or -1, which corresponds to the phase shift of 0 or  $\pi$ . In this scheme, the diagonals of all possible phase-shift matrices are composed of each column in a Hadamard matrix. It is worth noting that a  $U \times U$ -dimensional Hadamard matrix exists if and only if  $U \in \mathcal{H} = \{2\} \cup \{4i, i \in \mathbb{Z}^+\}$ . Therefore, the proposed Hadamard codebook based scheme is only valid for the number of IRS elements  $M \in \mathcal{H}$ . The case that  $M \notin \mathcal{H}$  leaves as our future works. The performance achieved by the Hadamard codebook based scheme is presented in Section V.

## V. NUMERICAL RESULTS

In this section, numerical examples are provided to validate our proposed designs. As illustrated in Fig. 2, an IRS-assisted multi-user communication system is considered, in which the AP and the IRS are located at  $(0, 0, 0)$  meters and  $(d_R, d_V, 0)$  meters, respectively. We consider

the case with  $K = 2$  users, whose locations are set as  $(d_1, 0, 0)$  meters and  $(d_2, 0, 0)$  meters. The distances for the direct link, the AP-IRS link and the IRS-user link are denoted by  $d_{D,k}$ ,  $d_{AI}$  and  $d_{I,k}$ , respectively. The distance-dependent path loss for all channels is modeled as  $PL(d) = \rho_0 \left(\frac{d}{d_0}\right)^{-\alpha}$ , where  $\rho_0 = -30$  dB denotes the path loss at the reference distance  $d_0 = 1$  meter ( $m$ ),  $d$  denotes the link distance and  $\alpha$  denotes the path loss exponent. We set  $d_1 = 20$  m,  $d_2 = 30$  m,  $d_R = 28$  m and  $d_V = 2$  m. For small scale fading, the Rayleigh fading channel model and the Rician fading model are assumed for the direct link and the AP-IRS/IRS-user links, respectively. Let  $K_{AI}$  and  $K_{IU}$  denote the Rician factors of the AP-IRS/IRS-user links. In this paper, the path loss exponents for the direct link, AP-IRS link and IRS-user link are set to be  $\alpha_D = 3.5$ ,  $\alpha_{AI} = 2.2$  and  $\alpha_{IU} = 2.8$ , respectively [15]. The Rician factors are  $K_{AI} = K_{IU} = 3$  dB. Each reflecting element of IRS is assumed to have a 3 dBi gain as the IRS reflects signals only in its front half-space. The noise power is set to be  $\sigma = -90$  dBm.

#### A. Ergodic Rate and Capacity Regions of IRS

In Fig. 3(a), we present the ergodic rate and capacity regions with 1-bit and 2-bit discrete phase shifts for a random realization of  $h_k, \mathbf{v}, \mathbf{g}_k$ . We set  $M = 8$  and  $P_{max} = 0$  dBm. The ergodic rate and capacity regions with the IRS are denoted by ‘‘E-IRS-OMA’’ and ‘‘E-IRS-NOMA’’, respectively. For comparison, we also provide the ergodic rate region of OMA with continuous phase shifts using the method in **Remark 3** and the rate and capacity regions without the IRS. It is first observed that the ergodic capacity region with the IRS is significantly larger than that without the IRS, which demonstrates the IRS performance advantages. For the two transmission schemes, the ergodic capacity region with NOMA outperforms the ergodic rate region with OMA. Both the rate and capacity regions are convex due to time-sharing. It is also observed that the ergodic rate and capacity region can be further improved by increasing the number of resolution bits  $B$  for the IRS, since a larger  $B$  results in a more accurate phase-shift matrix to

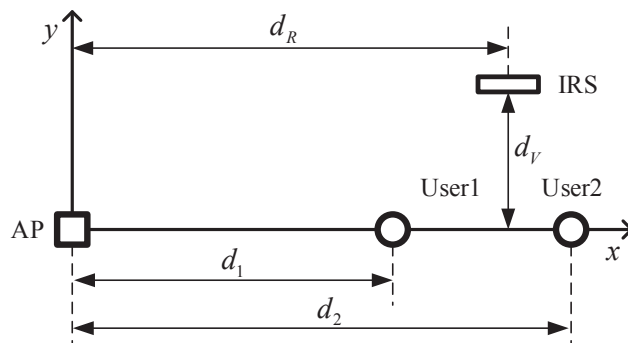


Fig. 2: The simulated IRS-assisted 2-user communication scenario.

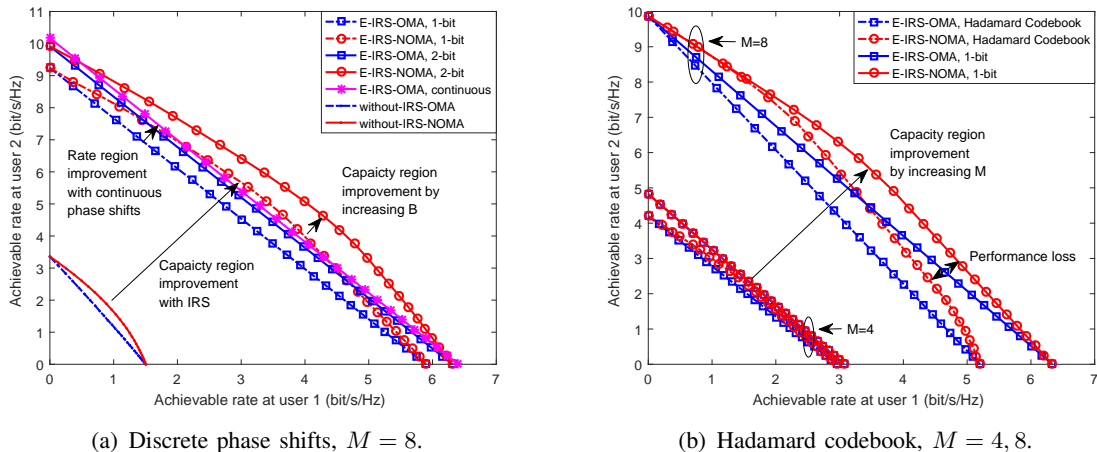


Fig. 3: Ergodic rate and capacity regions for a random realization of  $h_k, \mathbf{v}, \mathbf{g}_k$  with  $P_{max} = 0$  dBm.

enhance the performance. In particular, the performance gap between continuous phase shifts and 2-bit phase shifts is negligible, which implies that 2-bit phase shifts may serve as a promising candidate to achieve a desirable performance-complexity tradeoff. It is also observed that the ergodic capacity region of NOMA outperforms the OMA ergodic rate region with continuous phase shifts in some areas even if the IRS only has discrete phase shifts, which validates the advantages of NOMA.

In Fig. 3(b), we present the ergodic rate and capacity regions achieved by the Hadamard codebook. To evaluate the performance, the case of IRS with 1-bit phase shifts are provided. We set  $P_{max} = 0$  dBm and  $M = 4, 8$ . It is observed that the ergodic capacity regions are enlarged by increasing the number of IRS elements  $M$  because a higher array gain is achieved. When  $M = 4$ , the ergodic rate and capacity regions achieved by the Hadamard codebook are close to those of 1-bit phase shifts. However, the performance loss becomes pronounced when  $M = 8$ . This is expected since the size of all possible IRS phase-shift matrices grows exponentially with  $M$ , i.e.,  $L^M$ , while the size of Hadamard codebook only linearly increases with  $M$ . Though suffering from the performance loss, the Hadamard codebook based scheme enjoys a lower complexity and serves as a lower bound on the optimal performance gains.

### B. Delay-limited Rate and Capacity Regions of IRS

In Fig. 4(a), we present the delay-limited rate and capacity regions with 1-bit and 2-bit discrete phase shifts for a random realization of  $h_k, \mathbf{v}, \mathbf{g}_k$  with  $M = 8$  and  $P_{max} = 0$  dBm. The delay-limited rate and capacity regions with the IRS are denoted by ‘‘E-IRS-OMA’’ and ‘‘E-IRS-NOMA’’, respectively. Similarly, the rate and capacity regions without the IRS are provided for comparison. As expected, the delay-limited rate and capacity regions are also enlarged by



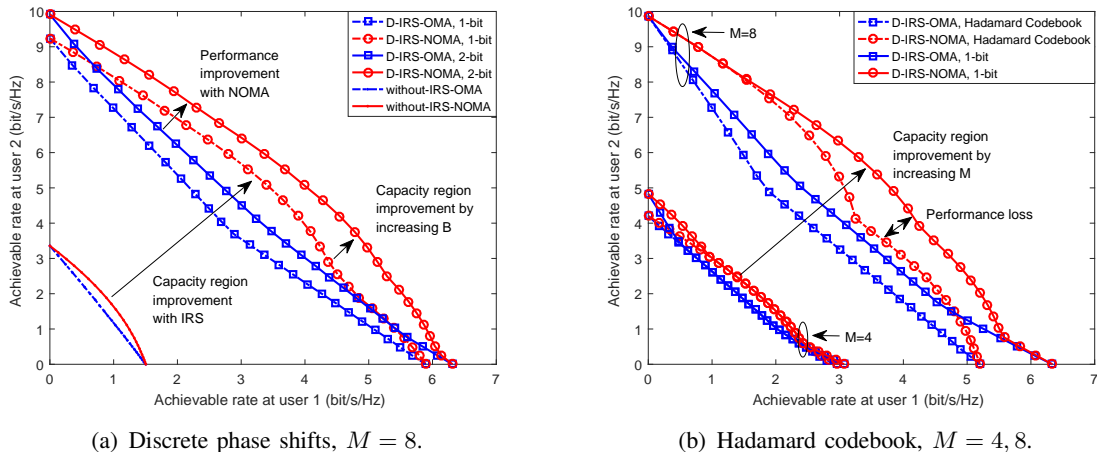


Fig. 4: Delay-limited rate and capacity regions for a random realization of  $h_k, \mathbf{v}, \mathbf{g}_k$  with  $M = 4, 8$  and  $P_{max} = 0$  dBm.

introducing the IRS and further improved with higher resolution bits. However, the delay-limited rate and capacity regions are all non-convex. This is because the IRS phase-shift matrix should be fixed with different values for different rate-profile  $\alpha$ .

In Fig. 4(b), we also compare the delay-limited rate and capacity regions achieved by the Hadamard codebook based scheme and 1-bit phase shifts. Similarly, increasing the number of IRS elements  $M$  is capable of improving the delay-limited rate and capacity regions due to the higher array gains. Compared with the ergodic capacity in Fig. 3(b), the performance loss of the Hadamard codebook based scheme in the delay-limited capacity becomes more severe since the IRS phase cannot be dynamically adjusted.

### C. Sum Rate Performance Comparison

In this subsection, we compare the sum rate performance of our proposed designs with the following benchmark schemes:

- **IRS OMA equal:** The AP serves two users with the aid of the IRS, where the time/frequency resources are equally allocated. In this case, the sum rate is maximized by only optimizing the power allocation among users.
- **without IRS:** The AP serves two users without the aid of an IRS. In this case, the sum rate is maximized by solving a conventional resource allocation problem with OMA and NOMA schemes.

The sum rate performances of ergodic and delay-limited capacity cases are obtained with the Hadamard codebook. We set  $\alpha_1 = \alpha_2 = 0.5$ . All results in Fig. 5 and Fig. 6 are averaged over 100 independent channel realizations.

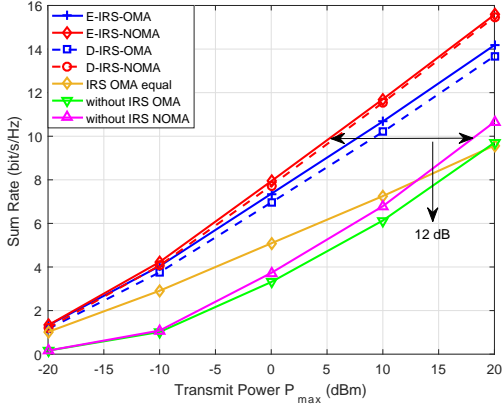


Fig. 5: The sum rate versus transmit power  $P_{max}$  with  $M = 8$ .

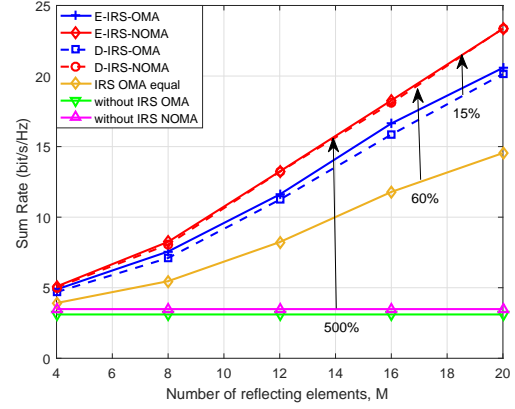


Fig. 6: The sum rate versus  $M$  with  $P_{max} = 0$  dBm.

1) *Sum Rate versus Transmit Power  $P_{max}$* : Fig. 5 shows the sum rate performance versus the maximum transmit power  $P_{max}$  with different schemes and  $M = 8$ . It is observed that for all schemes, the sum rate performances increase with  $P_{max}$ . Our proposed schemes significantly outperform other benchmark schemes. In addition, NOMA is capable of achieving a higher sum rate performance than OMA in each scheme. Moreover, the ergodic sum rate outperforms the delay-limited sum rate especially for the OMA scheme. This is because delay-tolerant transmission allows the IRS phase to be dynamically adjusted, which increases the degree-of-freedom (DoF) to enhance the performance. It is also observed that the “IRS OMA equal” scheme only outperforms the “without IRS” scheme for lower transmit power. Although assisted by the IRS, the “IRS OMA equal” scheme achieves the worst performance as  $P_{max}$  increases due to the fixed resource allocation scheme. This validates the importance of resource allocation optimization.

2) *Sum Rate versus the Number of IRS Elements  $M$* : Fig. 6 depicts the sum rate performance versus the IRS elements number  $M$  with different schemes and  $P_{max} = 0$  dBm. It is first observed that for all IRS-assisted schemes, as  $M$  increases, the sum rate performances increase, while the performance of the “without IRS” scheme remains unchanged. In particular, the performance gain brought by the IRS becomes more pronounced as  $M$  increases due to the higher achieved array gain. It is worth pointing out that the performance gain of NOMA over OMA in the proposed IRS-assisted scheme is more noticeable than that in the “without IRS” scheme. This is because the IRS is capable of enlarging the channel gain disparity among users, where NOMA can achieve a higher performance gain than OMA.

## VI. CONCLUSION

In this paper, we investigated an IRS-assisted multi-user communication system, where a single-antenna AP sends independent information to multiple single-antenna users with the aid of a discrete phase shifts IRS. Under this setup, we jointly optimized the IRS phase-shift matrix and resource allocation to reveal the fundamental rate limits of the IRS-assisted system with OMA and capacity-achieving NOMA transmission schemes. In particular, we considered the two cases: ergodic capacity and delay-limited capacity. For each case, we optimally solve the formulated Pareto boundary characterization problems with convex optimization techniques. It is shown that the optimal transmission strategy for achieving the ergodic capacity follows the alternative transmission strategy with dynamically changing IRS phase shifts. However, for achieving the delay-limited capacity, the IRS phase-shift matrix should be fixed with a specific value. Numerical results showed the significant ergodic and delay-limited capacity gains can be achieved by deploying the IRS compared with other benchmark schemes. Capacity characterization of the IRS-assisted multi-user communication system with conventional fading channels or multi-antenna AP/receivers are left for our future works.

### APPENDIX A: PROOF OF LEMMA 2

Under a given IRS phase-shift matrix  $\Theta$ , we can re-express each subproblem in (10) as

$$\max_{\{p_k, \omega_k\}} \sum_{k=1}^K \frac{\lambda_k^{ave,O}}{T} \omega_k \log_2 \left( 1 + \frac{|h_k + \mathbf{g}_k^H \Theta \mathbf{v}|^2 p_k}{\omega_k \sigma^2} \right) \quad (43a)$$

$$\text{s.t.} \quad \sum_{k=1}^K p_k \leq P_{max}, \quad (43b)$$

$$\sum_{k=1}^K \omega_k \leq 1, \quad (43c)$$

$$p_k \geq 0, 0 \leq \omega_k \leq 1, \forall k, \quad (43d)$$

Define  $\omega_k \log_2 \left( 1 + \frac{|h_k + \mathbf{g}_k^H \Theta \mathbf{v}|^2 p_k}{\omega_k \sigma^2} \right) \triangleq 0$  when  $\omega_k = 0, \forall k$ , such that the objective function of (43a) is jointly concave with respect to  $\omega_k$  and  $p_k$ . Therefore, problem (43) is a convex problem, we apply the Lagrangian dual method to optimally solve it. New non-negative Lagrange multipliers  $\delta^{ave,O}$  and  $\nu^{ave,O}$  are introduced associated with constraints (43b) and (43c), respectively. For given  $\delta^{ave,O}$  and  $\nu^{ave,O}$ , the Lagrange dual function of problem (43) can be expressed by

$$\max_{\{p_k, \omega_k\}} \mathcal{L}_4(\{p_k\}, \{\omega_k\}, \delta^{ave,O}, \nu^{ave,O}) \quad (44a)$$

$$\text{s.t.} \quad (43d), \quad (44b)$$

where  $\mathcal{L}_4(\{p_k\}, \{\omega_k\}, \delta^{ave,O}, \nu^{ave,O}) = \sum_{k=1}^K \frac{\lambda_k^{ave,O}}{T} \omega_k \log_2 \left( 1 + \frac{|h_k + \mathbf{g}_k^H \Theta \mathbf{v}|^2 p_k}{\omega_k \sigma^2} \right) - \delta^{ave,O} \sum_{k=1}^K p_k - \nu^{ave,O} \sum_{k=1}^K \omega_k$ .

Note that the problem (44) is jointly concave with respect to  $\omega_k$  and  $p_k$ , hence, the Karush-Kuhn-Tucker (KKT) conditions are necessary and sufficient for the optimality of (44). By taking the derivative of the objective function of (44) with respect to  $p_k^*$ , the optimal power allocation structure to (44) under given  $\delta^{ave,O}$  and  $\nu^{ave,O}$  proves to be  $p_k^* = \omega_k^* t_k^{ave,O}, \forall k$ , where  $t_k^{ave,O} = \left( \frac{\lambda_k^{ave,O}}{\delta^{ave,O} T \ln 2} - \frac{\sigma^2}{|h_k + \mathbf{g}_k^H \Theta \mathbf{v}|^2} \right)^+$ . Though the optimal values of  $p_k^*$  and  $\omega_k^*$  are coupled, the value of  $t_k^{ave,O}$  is uniquely determined by the dual variables. By substituting  $p_k^*$  into (43), we get

$$\max_{\{\omega_k\}} \sum_{k=1}^K \omega_k g_k \left( t_k^{ave,O} \right) \quad (45a)$$

$$\text{s.t.} \quad \sum_{k=1}^K \omega_k \leq 1, 0 \leq \omega_k \leq 1, \forall k, \quad (45b)$$

where  $g_k \left( t_k^{ave,O} \right) = \frac{\lambda_k^{ave,O}}{T} \log_2 \left( 1 + \frac{|h_k + \mathbf{g}_k^H \Theta \mathbf{v}|^2 t_k^{ave,O}}{\sigma^2} \right)$ . It is evident that problem (45) is a LP whose optimal solutions are given by

$$p_k^* = \begin{cases} \left( \frac{\lambda_k^{ave,O}}{\delta^{ave,O} T \ln 2} - \frac{\sigma^2}{|h_k + \mathbf{g}_k^H \Theta \mathbf{v}|^2} \right)^+, & \text{if } k = k^* \\ 0, & \text{otherwise} \end{cases}, \omega_k^* = \begin{cases} 1, & \text{if } k = k^* \\ 0, & \text{otherwise} \end{cases}$$

where  $k^* = \arg \max_{k \in \mathcal{K}} g_k \left( t_k^{ave,O} \right)$ , which indicates that there is only one user served at the optimal solution. By updating  $\delta^{ave,O}$  until  $p_k^* = P_{max}$ , the optimal  $\{p_k^*, \omega_k^*\}$  to problem (43) under given  $\Theta$  is achieved among  $\{(\mathbf{0}_{k-1}, P_{max}, \mathbf{0}_{K-k}), (\mathbf{0}_{k-1}, 1, \mathbf{0}_{K-k}), \forall k\}$  leading to a larger objective value. It is evident that the optimal IRS phase-shift matrix for the  $k$ th solution should satisfy  $\Theta_k = \arg \max_{\Theta \in \mathcal{S}} |h_k + \mathbf{g}_k^H \Theta \mathbf{v}|^2, \forall k$ . Hence, we complete the proof for Lemma 2.

#### APPENDIX B: PROOF OF PROPOSITION 2

For the three user case, we first consider the scenario where there is only one active user and the maximum of  $\phi(\{\lambda_k^{ave,N}\}, \Theta) (\{q_k\})$  is achieved on the vertexes of  $\Psi$  as  $(P_{max}, 0, 0)_{\{1\}}, (P_{max}, P_{max}, 0)_{\{2\}}, (P_{max}, P_{max}, P_{max})_{\{3\}}$  where the subscript represents the index of active user.

Next, when there are two active users, the constraint on power allocation becomes  $P_{max} = q_j > q_k > 0, \forall j < k \in \mathcal{K}$ . Now, the maximum of  $\phi(\{\lambda_k^{ave,N}\}, \Theta) (\{q_k\})$  is achieved at the stationary point  $\bar{q}_k$ . Then, we obtain (23) by solving  $\nabla_{q_k} \phi(\{\lambda_k^{ave,N}\}, \Theta) (\{q_k\}) = 0$ . The stationary points for two active users are  $(P_{max}, P_{max}, \bar{q}_3)_{\{2,3\}}, (P_{max}, \bar{q}_2, 0)_{\{1,2\}}, (P_{max}, \bar{q}_3, \bar{q}_3)_{\{1,3\}}$ .

Then, for the general three active users case, the constraint on power allocation becomes  $P_{max} = q_1 > q_2 > q_3 > 0$ . The corresponding stationary point is  $(P_{max}, \bar{q}_2, \bar{q}_3)_{\{1,2,3\}}$ .

Hence, the proof of Proposition 2 with three users is completed. The proof for two users is similar and we omit for brevity.

## REFERENCES

- [1] X. Mu, Y. Liu, L. Guo, J. Lin, and N. Al-Dhahir, "Ergodic capacity characterization of IRS-assisted NOMA systems," in *Proc. IEEE ICC Workshop*, 2020.
- [2] W. Saad, M. Bennis, and M. Chen, "A vision of 6G wireless systems: Applications, trends, technologies, and open research problems," *IEEE Network*, pp. 1–9, 2019.
- [3] J. G. Andrews, S. Buzzi, W. Choi, S. V. Hanly, A. Lozano, A. C. K. Soong, and J. C. Zhang, "What will 5G be?" *IEEE J. Sel. Areas Commun.*, vol. 32, no. 6, pp. 1065–1082, June 2014.
- [4] Q. Wu and R. Zhang, "Towards smart and reconfigurable environment: Intelligent reflecting surface aided wireless network," *IEEE Commun. Mag.*, pp. 1–7, 2019.
- [5] Y. Liang, R. Long, Q. Zhang, J. Chen, H. V. Cheng, and H. Guo, "Large intelligent surface/antennas (LISA): Making reflective radios smart," *J. Commun. Inf. Networks*, pp. 1–7, 2019.
- [6] E. Basar, M. Di Renzo, J. De Rosny, M. Debbah, M. Alouini, and R. Zhang, "Wireless communications through reconfigurable intelligent surfaces," *IEEE Access*, vol. 7, pp. 116 753–116 773, 2019.
- [7] Y. Cai, Z. Qin, F. Cui, G. Y. Li, and J. A. McCann, "Modulation and multiple access for 5G networks," *IEEE Commun. Surv. Tut.*, vol. 20, no. 1, pp. 629–646, Firstquarter 2018.
- [8] Z. Ding, Y. Liu, J. Choi, Q. Sun, M. Elkashlan, C. I, and H. V. Poor, "Application of non-orthogonal multiple access in LTE and 5G networks," *IEEE Commun. Mag.*, vol. 55, no. 2, pp. 185–191, February 2017.
- [9] Y. Liu, Z. Qin, M. Elkashlan, Z. Ding, A. Nallanathan, and L. Hanzo, "Nonorthogonal multiple access for 5G and beyond," *Proc. IEEE*, vol. 105, no. 12, pp. 2347–2381, Dec 2017.
- [10] Q. Wu and R. Zhang, "Intelligent reflecting surface enhanced wireless network via joint active and passive beamforming," *IEEE Trans. Wireless Commun.*, vol. 18, no. 11, pp. 5394–5409, Nov 2019.
- [11] C. Huang, A. Zappone, G. C. Alexandropoulos, M. Debbah, and C. Yuen, "Reconfigurable intelligent surfaces for energy efficiency in wireless communication," *IEEE Trans. Wireless Commun.*, vol. 18, no. 8, pp. 4157–4170, Aug 2019.
- [12] J. Chen, Y. Liang, Y. Pei, and H. Guo, "Intelligent reflecting surface: A programmable wireless environment for physical layer security," *IEEE Access*, vol. 7, pp. 82 599–82 612, 2019.
- [13] X. Yu, D. Xu, Y. Sun, D. W. K. Ng, and R. Schober, "Robust and secure wireless communications via intelligent reflecting surfaces," [Online]. Available:<https://arxiv.org/abs/1912.01497>.
- [14] Y. Yang, S. Zhang, and R. Zhang, "IRS-enhanced OFDMA: Joint resource allocation and passive beamforming optimization," [Online]. Available:<https://arxiv.org/abs/1912.01228>.
- [15] S. Zhang and R. Zhang, "Capacity characterization for intelligent reflecting surface aided MIMO communication," [Online]. Available:<https://arxiv.org/abs/1910.01573>.
- [16] T. Hou, Y. Liu, Z. Song, X. Sun, Y. Chen, and L. Hanzo, "MIMO assisted networks relying on large intelligent surfaces: A stochastic geometry model," [Online]. Available:<https://arxiv.org/abs/1910.00959>.
- [17] L. Dai, B. Wang, M. Wang, X. Yang, J. Tan, S. Bi, S. Xu, F. Yang, Z. Chen, M. Di Renzo, and L. Hanzo, "Reconfigurable intelligent surface-based wireless communication: Antenna design, prototyping and experimental results," [Online]. Available:<https://arxiv.org/abs/1912.03620>.
- [18] Z. Ding, P. Fan, and H. V. Poor, "Impact of user pairing on 5G nonorthogonal multiple-access downlink transmissions," *IEEE Trans. Veh. Technol.*, vol. 65, no. 8, pp. 6010–6023, Aug 2016.

- [19] Z. Chen, Z. Ding, X. Dai, and R. Zhang, "An optimization perspective of the superiority of NOMA compared to conventional OMA," *IEEE Trans. Signal Process.*, vol. 65, no. 19, pp. 5191–5202, Oct 2017.
- [20] Y. Liu, Z. Qin, M. ElKashlan, Y. Gao, and L. Hanzo, "Enhancing the physical layer security of non-orthogonal multiple access in large-scale networks," *IEEE Trans. Wireless Commun.*, vol. 16, no. 3, pp. 1656–1672, March 2017.
- [21] B. Wang, L. Dai, Z. Wang, N. Ge, and S. Zhou, "Spectrum and energy-efficient beamspace MIMO-NOMA for millimeter-wave communications using lens antenna array," *IEEE J. Sel. Areas Commun.*, vol. 35, no. 10, pp. 2370–2382, Oct 2017.
- [22] Y. Liu, Z. Qin, M. ElKashlan, A. Nallanathan, and J. A. McCann, "Non-orthogonal multiple access in large-scale heterogeneous networks," *IEEE J. Sel. Areas Commun.*, vol. 35, no. 12, pp. 2667–2680, Dec 2017.
- [23] Z. Ding and H. V. Poor, "A simple design of IRS-NOMA transmission," [Online]. Available:<https://arxiv.org/abs/1907.09918>.
- [24] G. Yang, X. Xu, and Y.-C. Liang, "Intelligent reflecting surface assisted non-orthogonal multiple access," [Online]. Available:<https://arxiv.org/abs/1907.03133>.
- [25] M. Fu, Y. Zhou, and Y. Shi, "Reconfigurable intelligent surface empowered downlink non-orthogonal multiple access," [Online]. Available:<https://arxiv.org/abs/1910.07361>.
- [26] X. Mu, Y. Liu, L. Guo, J. Lin, and N. Al-Dhahir, "Exploiting intelligent reflecting surfaces in multi-antenna aided NOMA systems," [Online]. Available:<https://arxiv.org/abs/1910.13636>.
- [27] J. Zhu, Y. Huang, J. Wang, K. Navaie, and Z. Ding, "Power efficient IRS-assisted NOMA," [Online]. Available:<https://arxiv.org/abs/1912.11768>.
- [28] T. Hou, Y. Liu, Z. Song, X. Sun, Y. Chen, and L. Hanzo, "Reconfigurable intelligent surface aided NOMA networks," [Online]. Available:<https://arxiv.org/abs/1912.10044>.
- [29] Wei Yu and R. Lui, "Dual methods for nonconvex spectrum optimization of multicarrier systems," *IEEE Trans. Commun.*, vol. 54, no. 7, pp. 1310–1322, July 2006.
- [30] D. Tse and P. Viswanath, *Fundamentals of Wireless Communication*. Cambridge, U.K.: Cambridge Univ. Press, 2005.
- [31] Lifang Li and A. J. Goldsmith, "Capacity and optimal resource allocation for fading broadcast channels .I. ergodic capacity," *IEEE Trans. Inf. Theory*, vol. 47, no. 3, pp. 1083–1102, March 2001.
- [32] M. Mohseni, Rui Zhang, and J. M. Cioffi, "Optimized transmission for fading multiple-access and broadcast channels with multiple antennas," *IEEE J. Sel. Areas Commun.*, vol. 24, no. 8, pp. 1627–1639, Aug 2006.
- [33] S. Boyd and L. Vandenberghe, *Convex Optimization*. Cambridge, U.K.: Cambridge Univ. Press, 2004.
- [34] M. Grant and S. Boyd, "CVX: Matlab software for disciplined convex programming, version 2.1," [Online]. Available:<http://cvxr.com/cvx>, Mar 2014.
- [35] S. Boyd, "Ellipsoid method," Stanford University. [Online]. Available:[https://web.stanford.edu/class/ee364b/lectures/ellipsoid\\_method\\_notes.pdf](https://web.stanford.edu/class/ee364b/lectures/ellipsoid_method_notes.pdf).
- [36] Lifang Li and A. J. Goldsmith, "Capacity and optimal resource allocation for fading broadcast channels .II. outage capacity," *IEEE Trans. Inf. Theory*, vol. 47, no. 3, pp. 1103–1127, March 2001.
- [37] H. Seleem, A. I. Sulyman, and A. Alsanie, "Hybrid precoding-beamforming design with hadamard RF codebook for mmwave large-scale MIMO systems," *IEEE Access*, vol. 5, pp. 6813–6823, 2017.